ACS OMEGA

Open Access

http://pubs.acs.org/journal/acsodf

Article

Transforming Agro-Industrial Waste into Bioplastic Coating Films

Diana Lucinda Castillo-Patiño, Humberto Geovani Rosas-Mejía, Alonso Albalate-Ramírez, Pasiano Rivas-García, Amanda Carrillo-Castillo, and José Rubén Morones-Ramírez*

Cite This: *ACS Omega* 2024, 9, 42970−42989

Read Online

ACCESS | Metrics & More | Article Recommendations

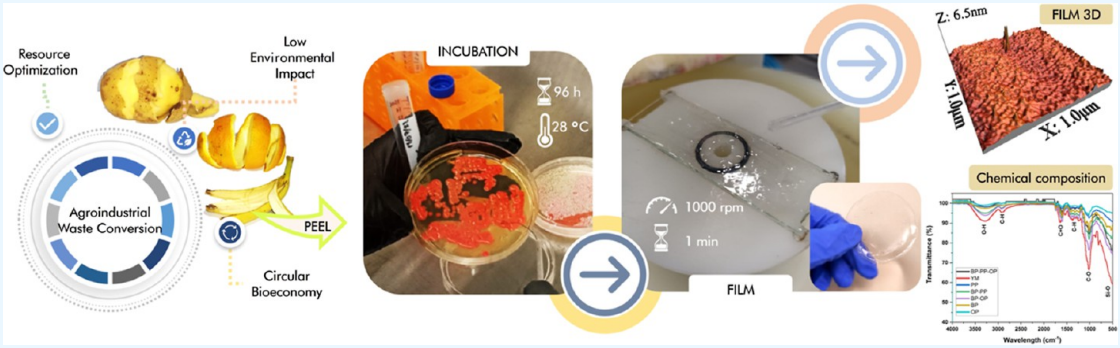

ABSTRACT: Addressing the environmental impact of agro-industrial waste, this study explores the transformation of banana, potato, and orange peels into bioplastics suitable for thin coating films. We prepared six extracts at 100 g/L, encompassing individual (banana peel, BP; orange peel, OP; and potato peel, PP) and combined [BP/OP, BP/PP, and BP/OP/PP] formulations, with yeast mold (YM) medium serving as the control. Utilizing the spin-coating method, we applied 1 mL of each sample at 1000 rpm for 1 min to create the films. Notably, the OP extract demonstrated a twofold increase in bioplastic yield (860.33 mg/L) compared to the yields of BP (391.43 mg/L), PP (357.67 mg/L), BP/OP (469.40 mg/L), BP/PP (382.50 mg/L), BP/OP/PP (272.67 mg/L), and YM (416.33 mg/L) extracts. Atomic force microscopy analysis of the film surfaces revealed a roughness under 8 nm, with the OP extract recording the highest at 7.0275 nm, whereas the BP/OP mixture exhibited the lowest roughness at 0.2067 nm and also formed the thinnest film at 6.5 nm. With R^2 trend values exceeding 0.9950, the films exhibited water vapor permeability values ranging from 3.05×10^{-3} to 4.44×10^{-3}, with the OP film being the least permeable and the BP/PP films the most permeable. The OP film demonstrated the lowest solubility in both water and ethanol with values of 64.71 and 1.05%, respectively. The solubilities of all films were above 60% in water and below 4% in ethanol. Furthermore, the films exhibited antimicrobial efficacy against both Gram-positive and Gram-negative bacteria. Our findings confirm the potential of utilizing banana, orange, and potato peels as viable substrates for eco-friendly bioplastics in thin-film applications.

1. INTRODUCTION

The pursuit of environmental sustainability has intensified the global effort to innovate in the management of agro-industrial waste. Inefficient valorization of such waste undermines ecological balance, economic value, and human health, and when incinerated or landfilled, it releases harmful compounds affecting local ecosystems.[1−3] Transforming these residues into bioplastics, with potential applications, presents a viable route to producing biodegradable materials, supporting eco-friendly industrial practices.[4,5]

The agroindustry, rich in organic byproducts like fruit peels and pulp, has untapped potential for repurposing waste into novel or enhanced products.[6−8] Specifically, banana, potato, and orange peels are promising due to their high content of natural polymers such as cellulose, starch, and lignin, making them suitable for bioplastics production and the synthesis of other bioactive compounds.[9−11] Advances in biotechnology have facilitated the development of efficient methods to convert such waste into biodegradable polymers, leveraging microbial synthesis.[12−14] The *Rhodotorula* genus comprises complex yeasts that are easy to grow and are highly efficient in transforming organic waste into valuable metabolites with industrial applications.[15−17] Specifically, *Rhodotorula mucilaginosa* UANL-001L, a native strain from northeastern Mexico, has shown remarkable potential in synthesizing biopolymers, from both commercial substrates and organic waste, with

Received: June 26, 2024
Revised: September 14, 2024
Accepted: September 24, 2024
Published: October 10, 2024

robust bioplastic properties, suitable for films and coatings.[18−20]

The replacement of synthetic polymers with bioplastics derived from renewable and abundant agro-industrial waste is a key research area.[21−23] In this context, this study applies the rotational coating technique to create thin bioplastic films from banana, potato, and OP extracts. The spin-coating method is chosen for its simplicity and effectiveness in controlling film thickness, offering a key advantage in terms of uniformity.[24,25] The preparation parameters—such as concentration, spin speed, distribution time, thickness, and drying temperature—are carefully optimized.[26−28] Surface topography is then meticulously characterized via atomic force microscopy (AFM), a technique critical for assessing nanoscale properties, such as roughness, grain size, distribution, thickness, and the fractal nature of the membranes.[29−32]

The use of banana, orange, and potato peels not only leverages their availability but also capitalizes on their polysaccharide-rich composition, suggesting their significant potential in synthesizing diverse bioplastic applications.[33−36] Hence, this article explores the conversion of banana, potato, and orange peels into bioplastics for thin-film applications. By reducing agro-industrial waste and curbing the environmental impact of plastic use, this research contributes to a more sustainable and economically viable future, aligning industry practices with environmental stewardship.

2. MATERIALS AND METHODS

2.1. Preparation of Agro-Industrial Waste Extracts. Agro-industrial residues consisting of banana, orange, and potato peels were sourced from horticultural companies and local merchants in Monterrey, Mexico. These were transported to the laboratory in Ziploc bags for subsequent processing. We prepared six extracts at a concentration of 100 g/L, which included individual extracts of banana peel (BP), orange peel (OP), and potato peel (PP) and their combinations (BP/OP, BP/PP, and BP/OP/PP). For each extract, 20 g of chopped peels was steeped in 200 mL of distilled water within 250 mL beakers. The mixtures were heated to 80 °C for 10 min on a hot plate and allowed to cool at ambient temperature for 20 min. The peels were prefiltered using gauze, and the resultant liquid was further clarified through a 2 μm cellulose filter (Whatman) using a Buchner funnel and vacuum pump. The filtered extracts were then transferred to 250 mL Erlenmeyer flasks and autoclaved at 121 °C for 15 min for sterilization.[19,37] Yeast mold (YM) broth was utilized as a control. All experimental procedures were replicated three times (n = 3).

2.2. Characterization of Extracts. The pH values of the extracts were measured by using an OHAUS potentiometer. Total solids were quantified via gravimetric analysis; specifically, 5 mL aliquots of each sample were dispensed into ceramic crucibles and desiccated at 105 °C for 2 h. Moisture content was calculated based on the mass difference before and after drying. Inorganic content or ash was determined by incinerating the dried samples in a muffle furnace at 550 °C for 30 min. Volatile solids were then calculated by subtracting the ash content from the total dried solids.[38,39]

Total nitrogen was assessed employing the Kjeldahl method (A.O.A.C 928.08, 1990), following the protocol described by Quintero-Curvelo et al. (2017)[39] and Florida-Rofner and Reategui-Diaz (2019).[40] The procedure involved digesting 5 g of the sample with 10 g of the Kjeldahl catalyst and 20 mL of 98% H_2SO_4, heating the mixture to 500 °C for 1 h. After digestion, 50 mL of 50% NaOH was introduced to neutralize the solution and convert ammonium ions to ammonia. The resulting ammonia was distilled and collected in 4% boric acid with a pH of 4.65 and titrated with HCl (0.25 mol/L) to quantify the nitrogen content. The percentage of nitrogen was calculated using the formula

$$\%\ \text{nitrogen} = (\text{mL HCl} - \text{mL blank}) \times N \text{ of HCl} \times 1.4007/\text{weight of the sample (g)}$$

2.3. Microbial Growth. The yeast *R. mucilaginosa* UANL-001L for this study was sourced from the Synthetic Biology and Systems Biology Laboratory at CIBYN, Monterrey, Mexico.[20] The strain was received on a solid culture medium. A single colony was taken, from a previously grown agar plate, with a sterile loop and inoculated into 10 mL of YM Difco (yeast malt broth) prepared according to the manufacturer's instructions. The culture was incubated for 24 h at 28 °C and 200 rpm agitation until reaching an $OD_{600\ nm}$ of 1. Subsequently, a 1% v/v inoculum was introduced to each peel extract, which was then incubated for 120 h under the same conditions. One milliliter samples were taken every 24 h to measure the yeast $OD_{600\ nm}$ in each extract using an OPTIZEN 2120 UV Plus spectrophotometer.

2.4. Determination of Reducing Sugars. The concentration of reducing sugars in the inoculated extracts was determined via the 3,5-dinitrosalicylic acid (DNS) colorimetric method.[41,42] A glucose calibration curve ranging from 0 to 5 g/L was prepared. Subsequently, 1 mL of each sample was centrifuged at 10,000 rpm for 5 min in a microcentrifuge (OHAUS FC5515), and 25 μL of the supernatant was reacted with 25 μL of the DNS reagent in a 1.5 mL Eppendorf tube, heated to 95 °C for 5 min, diluted with 250 μL of ultrapure water, and the absorbance was measured with a UV−vis spectrophotometer at a wavelength of 540 nm. Sugar quantification was determined at 24 h intervals, with a total of 6 readings at 0, 24, 48, 72, 96, and 120 h of microbial growth.

2.5. Elemental Evaluation of *R. mucilaginosa* UANL-001L Biomass. To assess the elemental composition of *R. mucilaginosa* UANL-001L biomass after 96 h of growth, 50 mL of the inoculated extract was taken in a Falcon tube and centrifuged at 10,000 rpm for 10 min to separate the biomass from the supernatant. The biomass was collected, washed three times with distilled water, and then lyophilized to remove the water content from the samples. Finally, the carbon, nitrogen, hydrogen, and sulfur content were quantified using a CHNS/O analyzer (PerkinElmer 2400).

2.6. Exopolysaccharide Extraction and Characterization. Exopolysaccharide [extracellular polymeric substance (EPS)] extraction followed the protocols described by Garza-Cervantes et al. (2019)[43] and Vazquez-Rodriguez et al. (2018).[20] *R. mucilaginosa* UANL-001L was incubated for 96 h at 28 °C and 200 rpm in the peel extracts from banana, orange, and potato. After the incubation period, the samples were centrifuged at 10,000 rpm for 20 min at 4 °C to recover the supernatant. The supernatant was passed through a 0.45 μm membrane filter (Millipore), and EPS was precipitated by adding 3 volumes of 96% ethanol per 1 volume of the filtered supernatant. The mixture was stored at −20 °C for 12 h and then centrifuged at 10,000 rpm for 20 min at 4 °C to recover the pellet. The pellet was washed three times with 70% ethanol

https://doi.org/10.1021/acsomega.4c05924
ACS Omega 2024, 9, 42970−42989

and dried for 5 h in a concentrator (SpeedVacSPD2010), preheated for 1 h at 45 °C.

2.7. Fourier-Transform Infrared Analysis of EPS. The identification of EPS functional groups from agro-industrial waste was achieved through Fourier-transform infrared spectroscopy (FTIR) analysis using a PerkinElmer spectrometer (Spectrum Two).

2.8. Preparation of Thin Bioplastic Films. Thin bioplastic films were prepared using the spin-coating technique.[44] EPS was first resuspended in 70% ethanol to achieve a concentration of 5 mg/mL. Subsequently, 1 mL of the EPS sample was added to a clean crystalline substrate and dispersed over the entire surface of the substrate using a rotational or centripetal force of 1000 rpm for 1 min. After spin coating, the films were subjected to a drying process at 70 °C for 5 min prior to further characterization.

2.9. Characterization of EPS Films. *2.9.1. Measurement of Surface Topography of Films, via AFM.* The surface morphology of the thin EPS films was characterized by using AFM (Park SYSTEMS NX10). The analysis was conducted in noncontact mode to preserve the integrity of the films, employing various scanning sizes to ensure comprehensive surface coverage.[30] Postacquisition, image processing was carried out with WSxM 4.0 Beta 9.3 software, which involved linear flattening for baseline correction and the transformation of raw data into three-dimensional representations to visualize and quantify surface features.

2.9.2. Water Vapor Permeability of EPS Films. The water vapor permeability (WVP) of the EPS films was evaluated by using a system designed to maintain equilibrium as constant as possible (Figure 1). For this purpose, an analytical balance

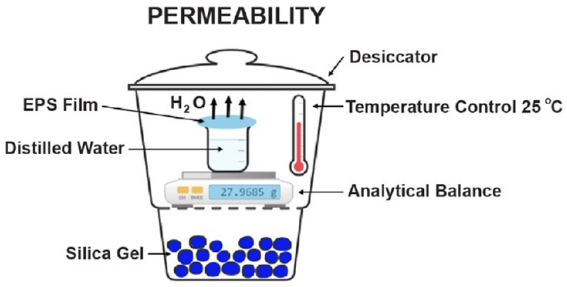

Figure 1. Schematic representation of the experimental setup used for measuring the WVP of the films.

with a precision of 0.0001 g was placed inside a desiccator containing silica gel. The EPS film was fixed to a wide-mouth 50 mL beaker (with an area of 1.134×10^{-3} m^2), which was prefilled with distilled water to 50% of its total capacity, and then placed on the balance inside the desiccator. A temperature sensor was installed within the desiccator to ensure precise temperature control at 25 °C, and the desiccator was securely sealed with its lid. Data were recorded at 30 min intervals over a span of 10 consecutive hours. The weight loss was plotted as a function of time (g/s), and the slope was determined through linear regression.[45,46] The WVP was calculated using the following equation

$$\mathrm{WVP} = (w/t) \times (x/\Delta P \times \mathrm{A})$$

where w/t (g/h) represents the mass of water permeated over time, x (mm) is the film thickness, A (m^2) is the exposed film area, and ΔP (Pa) is the water vapor pressure differential (3166 Pa at 25 °C).

2.9.3. Solubility of Films. The solubility of the films was evaluated in both water and absolute ethanol. The films were cut into square sections of 1.0 cm^2 and weighed to determine their initial dry mass. These sections were then immersed in the respective solvents and maintained under constant agitation at 180 rpm at 25 °C for a period of 6 h. After the immersion period, the unsolubilized portions were filtered and subsequently dried at 105 °C for 2 h.[47] The percentage of the soluble material was calculated using the following equation

$$\mathrm{WS}\ (\%) = [(W_0 - W_f)/W_0] \times 100$$

where WS (%) represents the water solubility, W_0 is the initial weight, and W_f is the final weight of the film. For ethanol solubility, the same formula was applied, substituting WS (%) for ES (%).

2.9.4. Antimicrobial Efficacy of EPS Films. The antimicrobial efficacy of EPS films was assessed by using zone of inhibition (ZOI) assays. Ten milliliters of LB (Luria−Bertani) broth were inoculated with a colony of the ATCC strains employed (*Escherichia coli* and *Staphylococcus aureus*) and incubated overnight at 37 °C. The cellular biomass was subsequently recovered by centrifugation at 10,000*g* for 5 min and washed with a phosphate-buffered saline solution, with shaking to enhance cell dispersion. The collected biomass was resuspended in 10 mL of medium and adjusted to an optical density of 1.0 at 600 nm (OD_{600} nm) using a UV−vis spectrophotometer, corresponding to a concentration equivalent to 3.95×10^8 CFU/mL. The bacterial suspensions were evenly spread over the surface of Petri dishes previously prepared with agar. The EPS films were applied to the plates in two methods: by depositing 10 μL of the film solution onto a sterile circular filter with a diameter of 6 mm and by directly placing films cut to the same diameter as the filter onto the inoculated agar, ensuring a distance of 2 cm between samples. The plates were incubated at 37 °C for 24 h, and the ZOI was

Table 1. Composition, Total Solid Profile, and Total Nitrogen Content in BP, OP, PP, BP/OP, BP/PP, and BP/OP/PP Extracts[a]

		characterization						
sample	composition (%)	pH	humidity (%)	total solids (%)	volatile S. (%)	ashes (%)	T. nitrogen (g N/g)	T. nitrogen (%)
BP	100	500	90.44 ± 0,06^a	9.56 ± 0,06^a	88.13 ± 0,95^a	11.87 ± 0,95^a	0.026 ± 0,01^a	2.6 ± 0,01^a
OP	100	400	94.5 ± 0,07^d	13.5 ± 0,07^b	96.2 ± 0,11^c	3.8 ± 0,11^c	0.010 ± 0,01^f	1.0 ± 0,01^f
PP	100	600	79.6 ± 0,08^c	20.4 ± 0,08^c	94.54 ± 0,17^b	5.46 ± 0,17^b	0.024 ± 0,00^e	2.4 ± 0,00^e
BP/OP	50/50	499	85.82 ± 1,24^b	14.18 ± 1,24^b	93.82 ± 0,68^b	6.17 ± 0,68^b	0.018 ± 0,01^c	1.8 ± 0,01^c
BP/PP	50/50	548	89.04 ± 0,33^a	10.96 ± 0,33^a	89.14 ± 0,35^a	10.86 ± 0,35^a	0.025 ± 0,02^b	2.5 ± 0,02^b
BP/OP/PP	50/25/25	524	86.87 ± 0, 92^b	13.13 ± 0,92^b	89.29 ± 0,47^a	10.70 ± 0,47^a	0.019 ± 0,01^d	1.9 ± 0,01^d

[a]No significant difference was found for equal letters ($P \geq 0.05$).

https://doi.org/10.1021/acsomega.4c05924
ACS Omega 2024, 9, 42970−42989

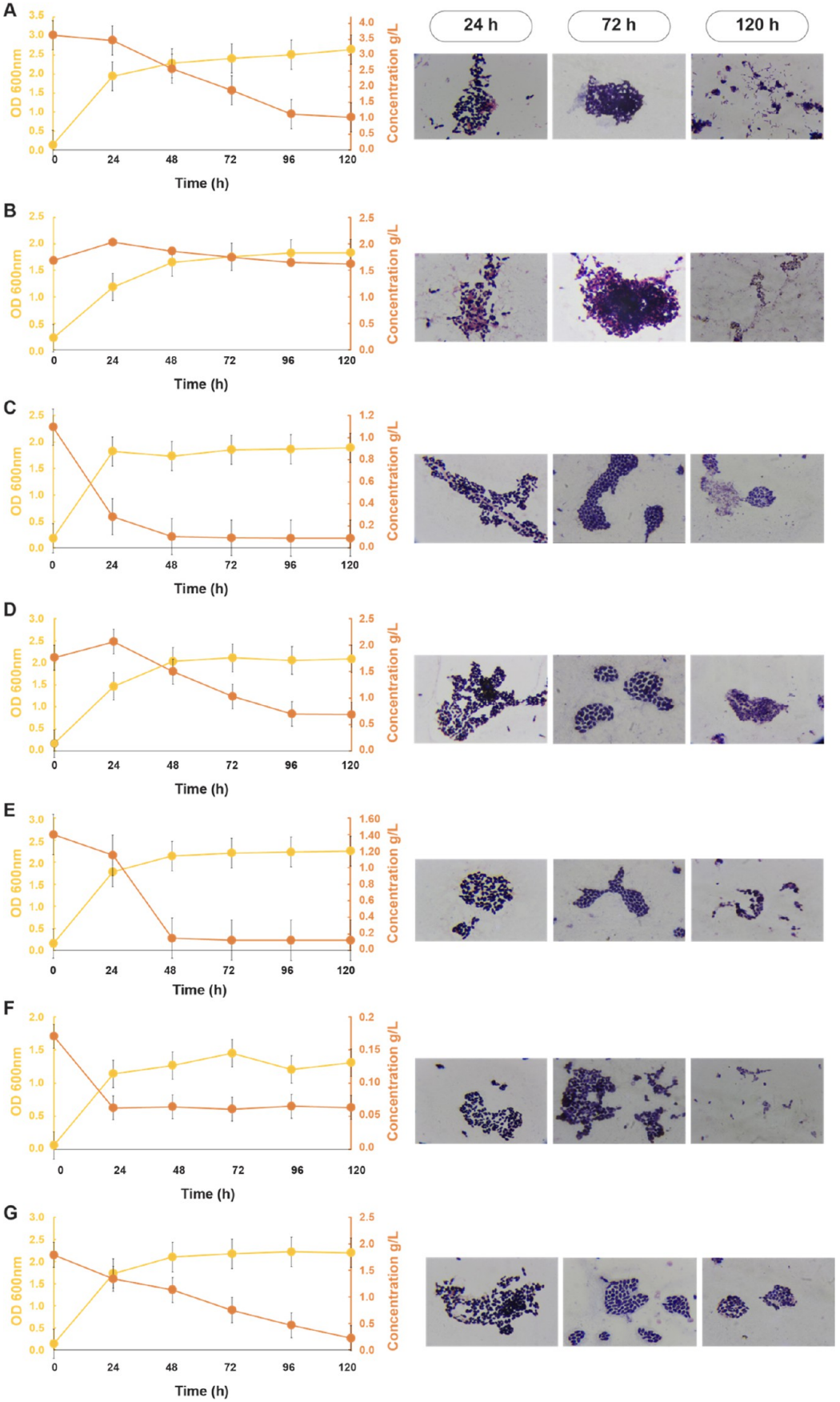

Figure 2. Growth kinetics, reducing sugar consumption and cell morphology of *R. mucilaginosa*UANL-001L in various media: (A) commercial YM medium; (B) BP extract; (C) BP/PP extract; (D) BP/OP extract; (E) BP/OP/PP extract; (F) PP extract; and (G) OP extract.

https://doi.org/10.1021/acsomega.4c05924
ACS Omega 2024, 9, 42970−42989

measured from two sides of the film circles to obtain an average value in millimeters.[45,48] All assays were performed in triplicate.

2.10. Statistical Analysis. For relevant assays, a one-way analysis of variance (ANOVA) was conducted, followed by Tukey's post hoc tests to determine statistically significant differences ($P < 0.05$) among the studied treatments.

Data obtained from the experimental assays were subjected to statistical scrutiny. A one-way ANOVA was performed to evaluate the differences among the groups. When ANOVA indicated significant differences, Tukey's post hoc test was employed to pinpoint which specific treatments differed from each other. A p-value of less than 0.05 was considered to indicate statistical significance.

3. RESULTS AND DISCUSSION

3.1. Proximal Characterization of Agro-Industrial Waste-Based Extracts. The concentration of 100 g/L for preparing the six agro-industrial waste-based extracts—namely, BP, OP, and PP at 100% pure, and combinations of BP/OP, BP/PP, and BP/OP/PP at ratios of 50/50%, 50/50%, and 50/25/25%, respectively (Table 1)—was selected based on the highest yield of exopolysaccharide (EPS) synthesis from BP as reported by Torres-Alvarez et al. (2022).[19] The pH levels of these extracts spanned from 4.0 in the OP extract to 6.0 in the PP extract. This range includes the BP, BP/OP, BP/PP, and BP/OP/PP media, which exhibited pH values of 5.0, 4.99, 5.48, and 5.24, respectively, aligning closely with the optimal growth pH of 5.0 for *R. mucilaginosa* UANL-001L. Furthermore, all extracts maintained pH levels within the permissible growth range (pH 4.0 to 6.5) for this yeast strain, supporting the viability of these media for microbial cultivation.[49,50]

Solid content and nitrogen levels within the media were quantified using gravimetric analysis and the Kjeldahl method, as shown in Table 1. Moisture content ranged from 79.6% in PP to 94.5% in OP, which is possibly attributable to the inherently lower solid content of citrus peels compared to potato waste.[51] In terms of total solids, the BP medium recorded the lowest at 9.56%, while the highest was noted for the PP medium at 20.4%. Volatile solids were most abundant in the OP extract, constituting 96.2% of its content, coupled with the smallest proportion of ash at 3.8%, reflecting its high organic matter content. Conversely, the BP extract contained the lowest proportion of volatile solids (88.13%) and the highest ash content (11.87%), indicative of a significant mineral presence, predominantly potassium and calcium.[52−54] The proximal composition of moisture, volatile solids, ash, and total nitrogen content of the OP extract was significantly different ($P < 0.05$) from the composition of the BP, PP, BP/OP, BP/PP, and BP/OP/PP extracts. However, a significant variation in total solid content was only observed in the PP medium.

The total Kjeldahl nitrogen content (Table 1) in our growth media varied, with values ranging from 0.010 ± 0.01 to 0.026 ± 0.01 g of N/g. The BP medium exhibited the highest nitrogen content, while the OP medium contained the least. Notably, the total nitrogen values for the PP extract and the combined BP/OP, BP/PP, and BP/OP/PP extracts were

Table 2. Available Monosaccharides in BP/PP, BP/OP, and BP/OP/PP Extracts after 96 h of Incubation

compound	retention time (min)	BP/PP	BP/OP	BP/OP/PP
maltose	11.8	279 mg/L	332 mg/L	308 mg/L
glucose	13.8	ND	ND	ND
xylose	14.7	ND	ND	ND
arabinose	16.39	ND	ND	ND
fructose	17.4	ND	1500 mg/L	ND
mannitol	25	ND	ND	ND
sorbitol	33.85	ND	ND	ND

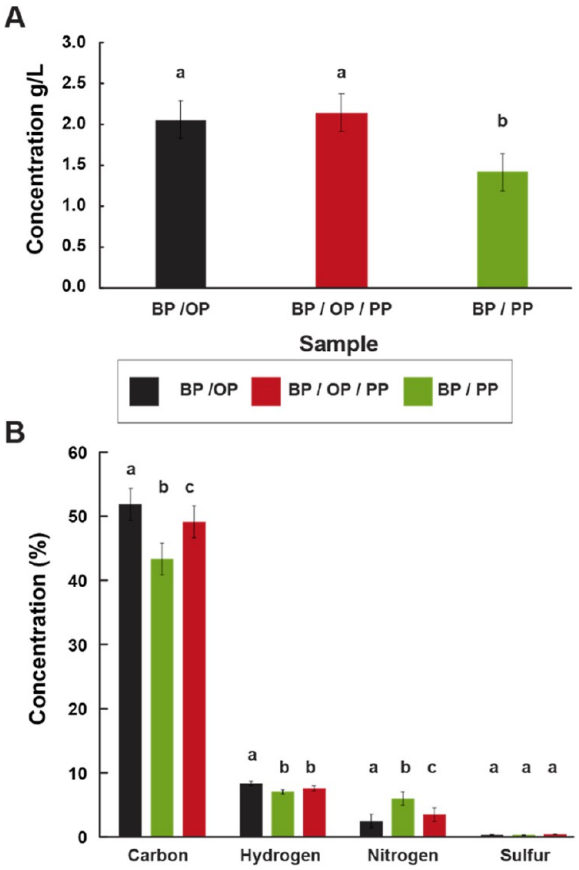

Figure 3. Quantitative analysis of biomass production and elemental composition: (A) biomass yield (g/L) obtained from *R. mucilaginosa* UANL-001L after 96 h of cultivation in combined extract media. (B) Elemental analysis showing the percentage of carbon (C), hydrogen (H), nitrogen (N), and sulfur (S) content in the biomass derived from the combined media. Different letters indicate statistically significant differences where $P < 0.05$, and similar letters denote no significant differences at $P \geq 0.05$.

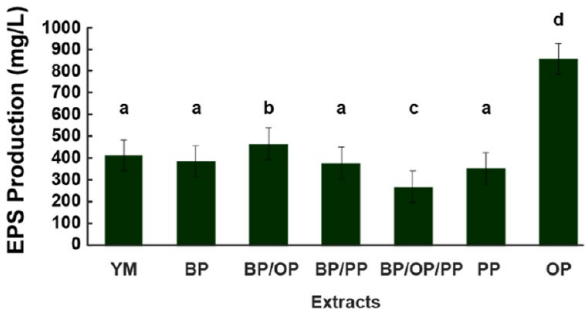

Figure 4. EPS production from banana, orange, and potato peels (*equal letters indicate no significant difference $P \geq 0.05$).

https://doi.org/10.1021/acsomega.4c05924
ACS Omega 2024, 9, 42970−42989

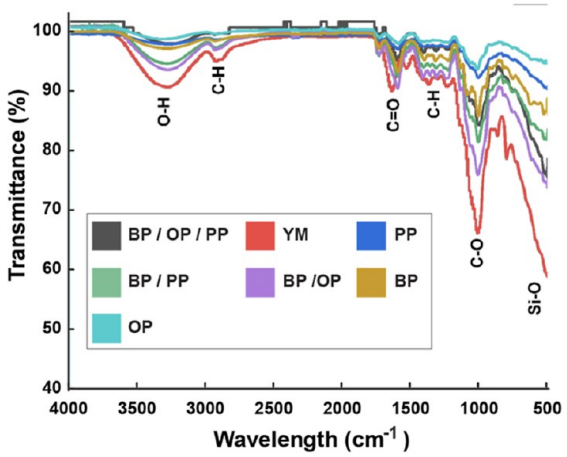

Figure 5. Spectra of peaks and labels of functional groups present in YM, BP, PP, OP, BP/OP, BP/PP, and BP/OP/PP EPS using FTIR.

recorded at 0.025 ± 0.02, 0.018 ± 0.01, 0.019 ± 0.01, and 0.024 ± 0.00 g N/g, respectively. These variations in total Kjeldahl nitrogen content among the media were statistically significant ($P < 0.05$). The nitrogen levels reported in this study align closely with the values documented in the literature,[55−58] reinforcing the reliability of our findings.

The strategic selection of extract concentrations and their pH calibration are pivotal for optimized microbial growth and metabolite production as they directly influence the bioavailability of nutrients and the environmental conditions conducive to yeast activity. The robustness of *R. mucilaginosa* UANL-001L across a range of pH levels suggests potential for its application in variable industrial waste streams, where pH can fluctuate. This adaptability could be harnessed to develop tailored bioprocessing strategies for converting waste into valuable products, potentially reducing the environmental footprint of agro-industrial operations.[59−61]

Moreover, the significant differences in total solid and nitrogen contents across the media not only reflect the compositional diversity of the waste materials but also highlight the need for a nuanced approach to medium preparation for microbial fermentation. The presence of high levels of volatile solids in the OP extract and the substantial

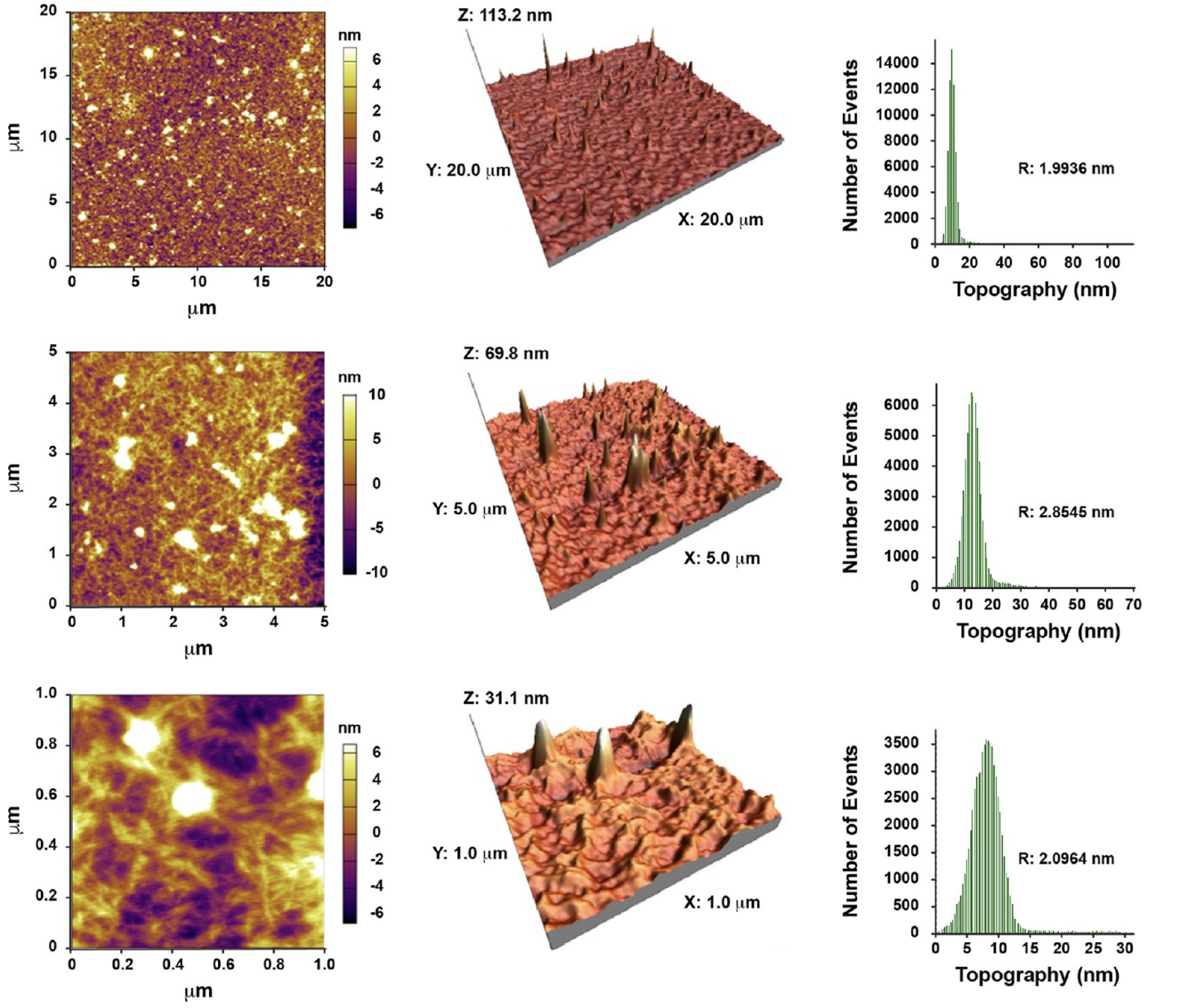

Figure 6. Morphology and topographical distribution of 2D and 3D AFM in the thin film of bioplastic BP.

https://doi.org/10.1021/acsomega.4c05924
ACS Omega 2024, 9, 42970−42989

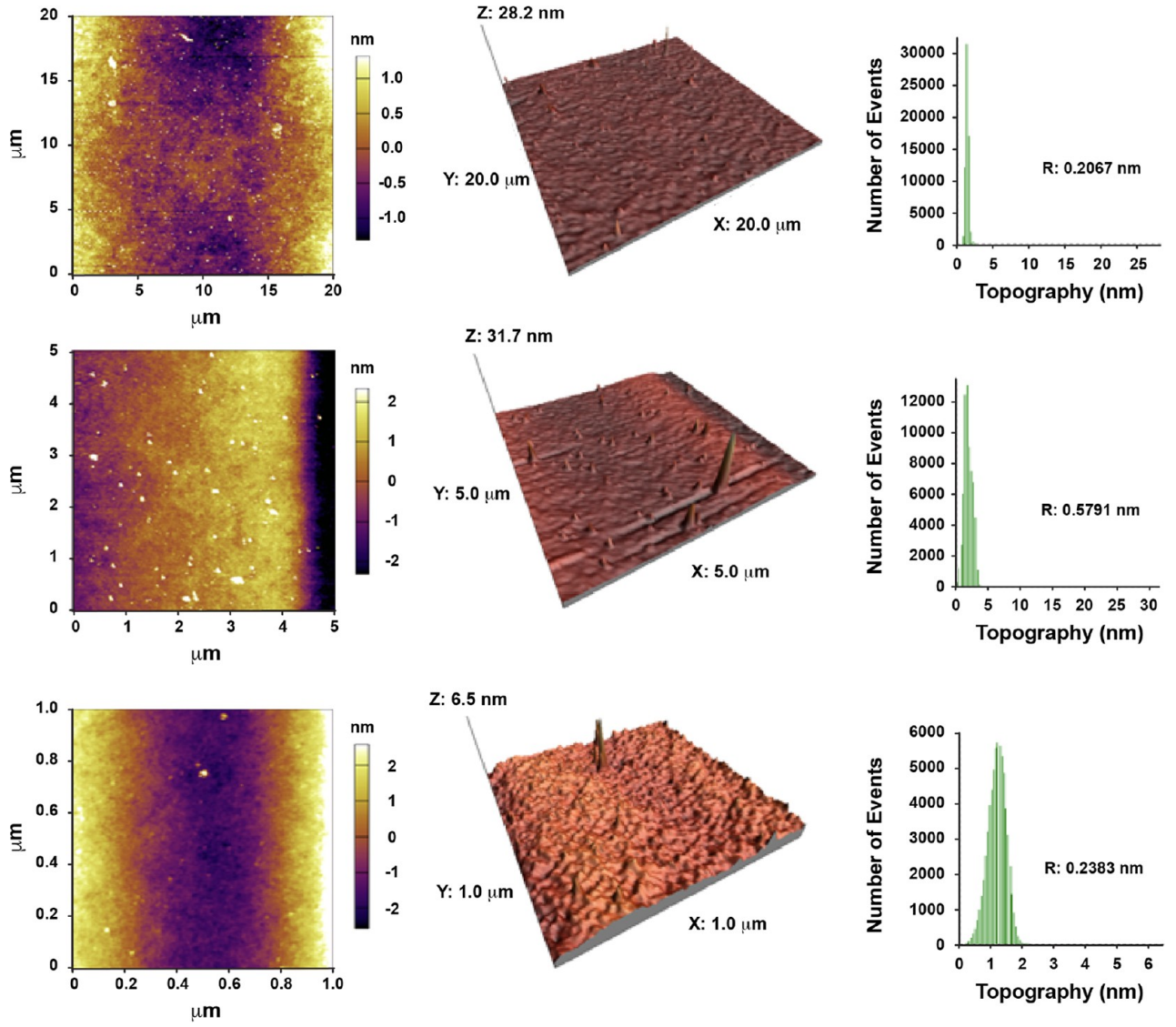

Figure 7. Morphology and AFM topographical distribution in 2D and 3D of the thin film of bioplastic BP/OP.

mineral content in BP extracts reveal the complex interplay between waste substrate characteristics and microbial nutrition. These insights open avenues for enhancing bioplastic production through selective waste valorization, where specific waste types could be matched with microbial strains to optimize the yield and properties of bioplastics.[62] The congruence of our findings with existing literature underlines the reproducibility and relevance of our approach, potentially contributing to more sustainable bioeconomy practices.

3.2. Growth Kinetics and Reducing Sugar Consumption of *R. mucilaginosa* UANL-001L. The efficacy of banana, orange, and potato-peel-derived media, along with their combined forms BP/OP, BP/PP, and BP/OP/PP, in supporting the growth of *R. mucilaginosa* UANL-001L, was evaluated through growth kinetics (OD at 600 nm), reducing sugar consumption (OD at 540 nm), and cell morphology (Gram staining) analyses (Figure 2). Growth comparisons were made against a commercially prepared YM medium, known for its optimal nutrient profile for *R. mucilaginosa* UANL-001L proliferation and high-value metabolite production.[20,49] Our results (Figure 2A−G) indicate that while *R. mucilaginosa* UANL-001L experienced robust growth in all tested peel media, it exhibited slightly lower growth compared to the commercial YM medium, particularly in the media derived from potato and banana peels (Figure 2B,F). Such growth patterns are likely reflective of the nutrient content and bioavailability in the extracts, which in turn affect the yeast's ability to adapt and grow optimally.[63,64]

In the growth analysis of *R. mucilaginosa* UANL-001L across the different culture media (Figure 2A−G), we observed a consistent pattern in its developmental phases. The yeast exhibited maximum growth within the initial 48 h period across all media types, followed by an entry into the stationary phase, peaking at 72 h. Postpeak, there was a notable decline in growth after 96 and 120 h of incubation, which aligns with the characteristic growth dynamics of *R. mucilaginosa*.[16,65] The maximum absorbances reached (OD 600 nm) in the treatments were 2.65 in YM; 1.83 in BP; 1.89 in BP/PP; 2.11 in BP/OP; 2.25 in BP/OP/PP; 1.45 in PP, and 2.22 in OP.

Concurrent with growth kinetics, the highest uptake of reducing sugars across all media types, including the YM control, was noted during the initial 48 h inoculation period with *R. mucilaginosa* UANL-001L (Figure 2A−G). Notably,

https://doi.org/10.1021/acsomega.4c05924
ACS Omega 2024, 9, 42970−42989

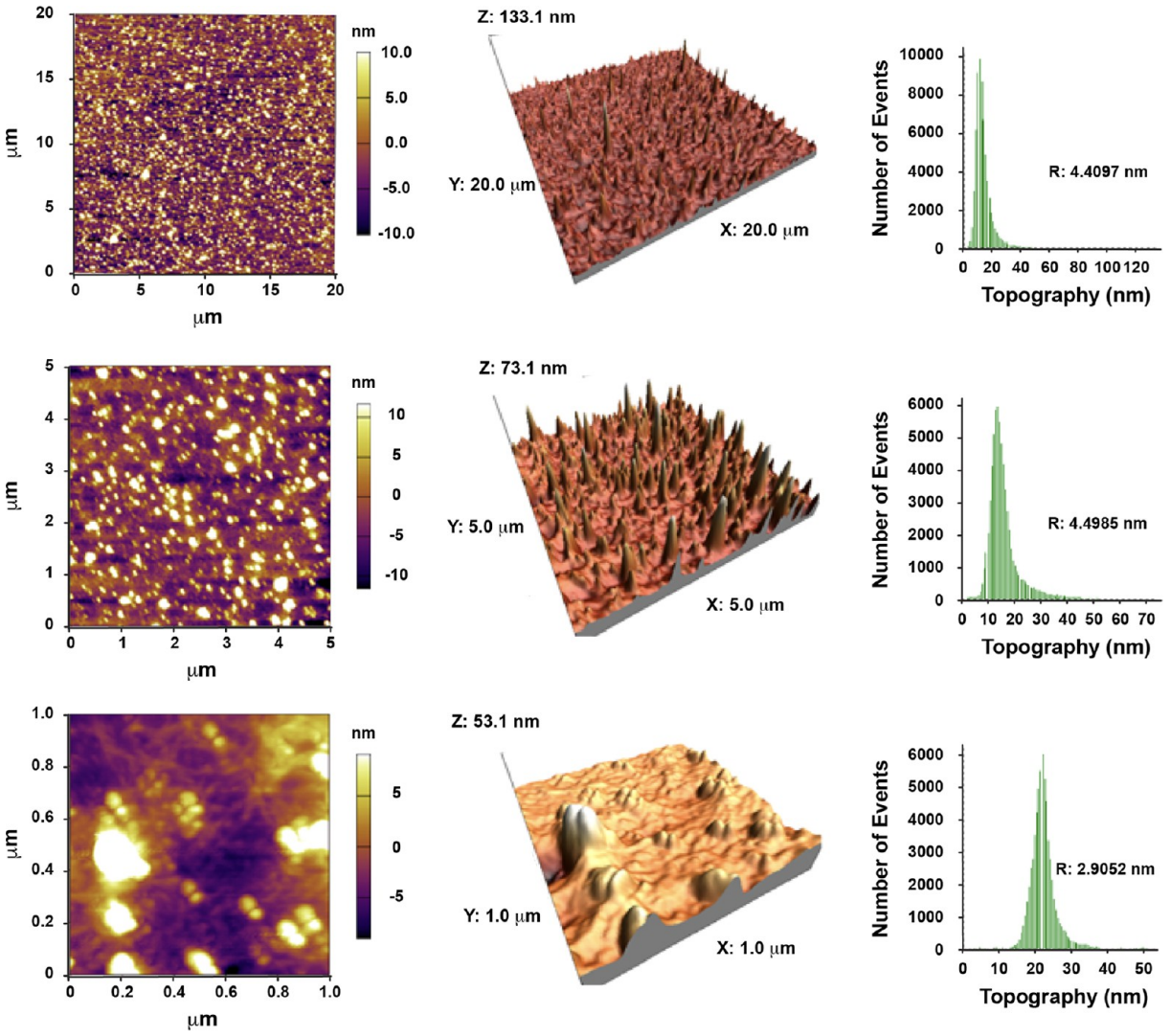

Figure 8. Morphology and AFM topographical distribution in 2D and 3D of the thin film of bioplastic BP/PP.

significant sugar utilization continued until 96 h in the BP, OP, BP/OP, and YM media (Figure 2A,B,D,G), after which no further consumption of reducing sugars was detected in any of the media. These observations align with other studies that have reported a predominant sugar consumption within the first 48 h of *R. mucilaginosa* growth.[19,66,67] It has been proposed that monosaccharides and disaccharides are preferentially utilized as carbon sources by *R. mucilaginosa*.[68,69] The extracts used in this study, derived from banana, orange, and potato peels, are rich in readily available sugars like glucose, fructose, and sucrose, which likely contributed to the observed efficient growth and metabolite synthesis by *R. mucilaginosa* UANL-001L.[70−74]

Gram staining facilitated the microscopic examination of *R. mucilaginosa* UANL-001L cell morphology at critical growth phases: exponential (24 h), stationary (72 h), and early decline (96 h) within each peel-based medium and the commercial YM (Figure 2A−G). The yeast cells exhibited typical spheroidal to oval blastoconidial morphology without hyphal structures and were surrounded by EPS, aligning with characteristics previously delineated for this species.[49,75] Cell development in YM, BP, PP, BP/PP, and BP/OP/PP media demonstrated a consistent pattern: an increase in cell density at 24 h, peaking at 72 h, followed by a decline at 96 h (Figure 2A−C,E,F). In contrast, the OP and BP/OP media sustained considerable cell concentrations at 96 h (Figure 2D,G), indicating potential variances in nutrient availability or utilization efficiency in these particular extracts.

The differential growth rates observed in *R. mucilaginosa* UANL-001L across various peel media offer insights into the intricate balance required between substrate composition and microbial metabolism for optimal bioprocesses. In addition, understanding the biochemical pathways responsible for the observed growth patterns could pave the way for genetic modifications that enhance the strain's efficiency in transforming agro-industrial waste to valuable bioproducts, a focus that aligns with the growing interest in sustainable biotechnology.[76]

Furthermore, the stationary phase dynamics and the sustained cell concentrations in OP and BP/OP media beyond the typical decline phase point to an underexplored robustness in *R. mucilaginosa* UANL-001L. This resilience, particularly in the face of varying sugar availabilities, underlines the yeast's potential for industrial fermentation processes that require prolonged cultivation periods. Future studies should delve into the metabolic adjustments the yeast undergoes in these

https://doi.org/10.1021/acsomega.4c05924
ACS Omega 2024, 9, 42970−42989

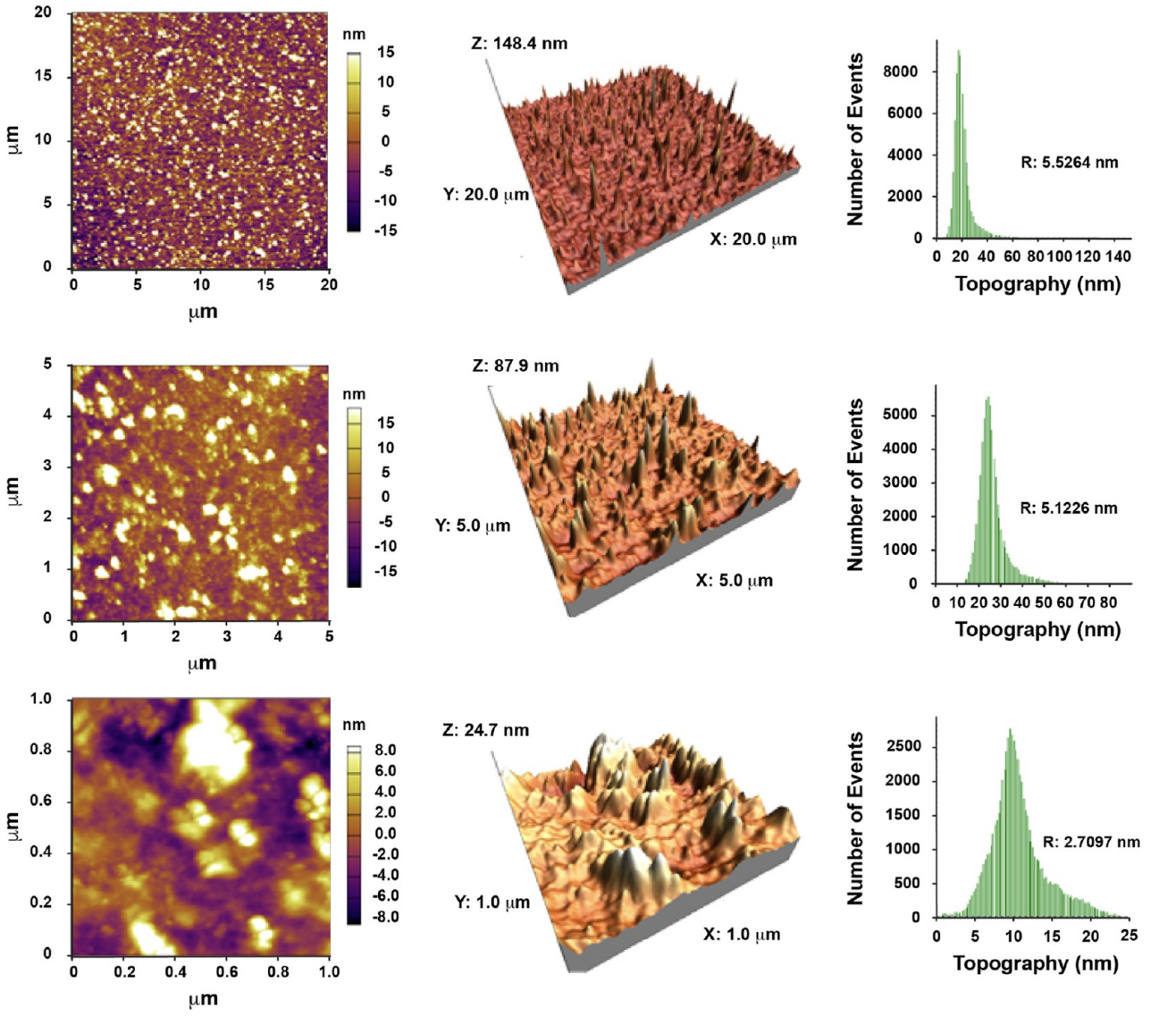

Figure 9. Morphology and AFM topographical distribution in 2D and 3D of the thin film of bioplastic BP/OP/PP.

substrates, which may reveal novel pathways for stress adaptation and long-term survival. Such knowledge could inform the development of specialized fermentation strategies for substrates with fluctuating sugar compositions, crucial for advancing circular economy approaches within the agro-industry.[77]

3.3. Available Monosaccharides in Combined Media. Monosaccharide analysis for the combined BP/PP, BP/OP, and BP/OP/PP media was conducted via pulsed amperometric detection following a 96 h incubation period, with findings detailed in Table 2. Maltose was consistently present across all media, suggesting that it was not fully utilized by *R. mucilaginosa* UANL-001L during the growth period. Interestingly, only the BP/OP medium showed the presence of fructose at a concentration of 1500 mg/L. The detectable levels of these sugars postincubation could reflect the abundant initial sugar content within the peel substrates, which presumably exceeded the assimilative capacity of *R. mucilaginosa*.[78,79]

The persistent presence of maltose in the substrate, even after a substantial incubation period, raises questions about the metabolic preferences of *R. mucilaginosa* UANL-001L and the enzymatic machinery involved in sugar uptake. The discovery of fructose only in the BP/OP medium also introduces the possibility of selective sugar utilization pathways that are influenced by the composition of the medium. This selectivity could be a result of the yeast's adaptive response to the unique nutrient profile of each medium or an indication of metabolic overflow, where the presence of a particular sugar suppresses the utilization of others. Further investigation into the transport and catabolism of different sugars by *R. mucilaginosa* could provide valuable insights for enhancing the efficiency of bioconversion processes, particularly in the context of industrial fermentation where maximizing substrate utilization is crucial.[80] Understanding these mechanisms could inform the engineering of more effective bioprocessing strategies that align with the principles of a circular economy, optimizing the use of renewable resources and reducing waste.

3.4. Elemental Composition of Biomass from BP/PP, BP/OP, and BP/OP/PP. Following a 96 h cultivation period, the generated biomass yields for *R. mucilaginosa* UANL-001L in the combined media of BP/PP, BP/OP, and BP/OP/PP were quantified at 1.42, 2.05, and 2.14 g/L, respectively, with the representation shown in Figure 3A. Notably, the BP/OP/

https://doi.org/10.1021/acsomega.4c05924
ACS Omega 2024, 9, 42970−42989

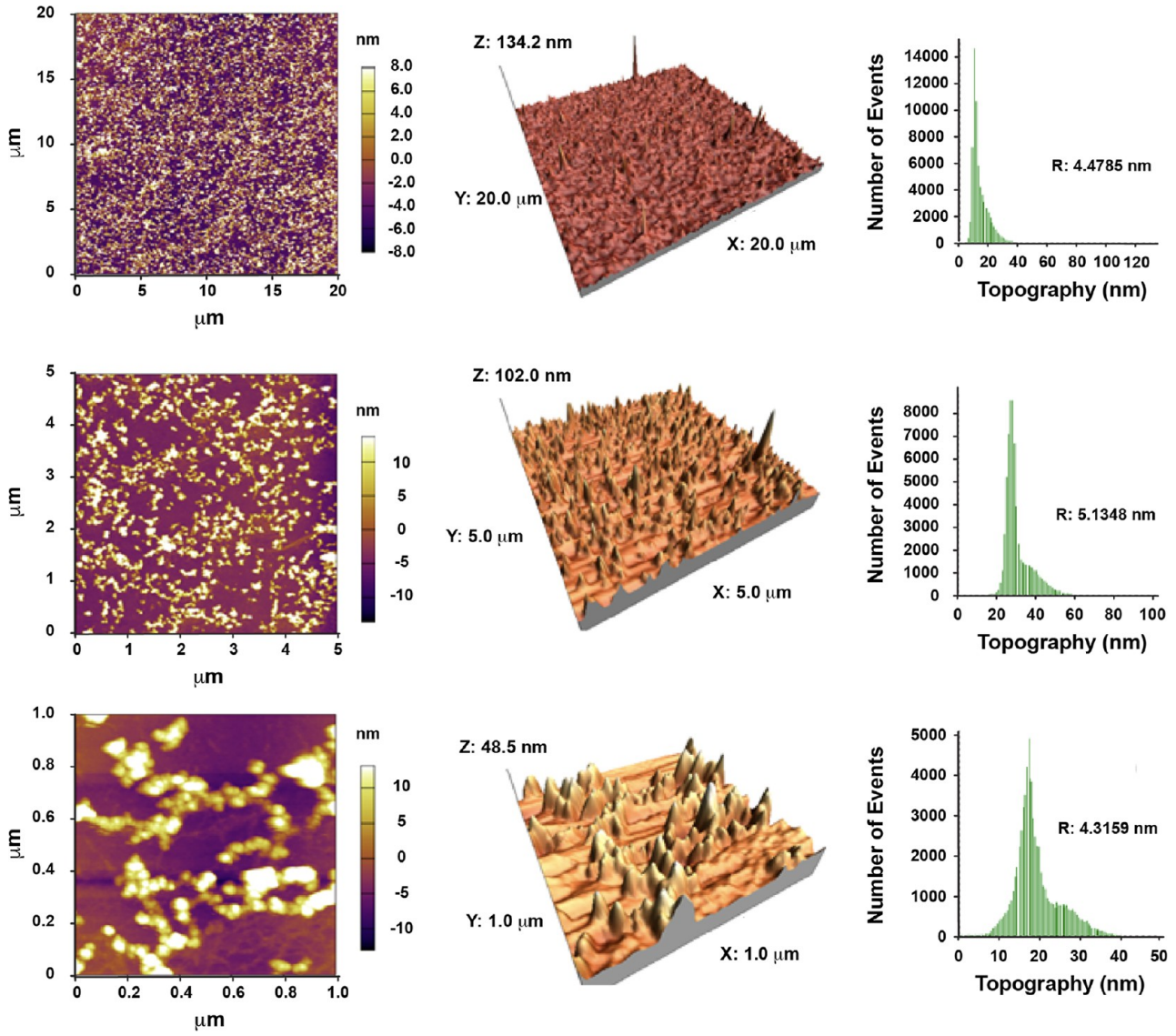

Figure 10. Morphology and AFM topographical distribution in 2D and 3D of the thin film of bioplastic PP.

PP medium resulted in the highest biomass production, peaking at 2.14 g/L. However, statistical analysis revealed that the biomass yield from the BP/PP medium was the only one to exhibit a significant difference (Figure 3A). These biomass production levels are consistent with the outcomes of similar studies utilizing YM and BP extracts as substrates for *R. mucilaginosa* UANL-001L biomass generation.[18,19,49]

Elemental composition of the dried biomass of *R. mucilaginosa* UANL-001L, recovered from the BP/PP, BP/OP, and BP/OP/PP media after 96 h of growth, was determined using a CHNS/O analyzer. The carbon content differed significantly across the media, with BP/PP at 43.37%, BP/OP at 51.90%, and BP/OP/PP at 49.14% ($P < 0.05$) (Figure 3B). A notable variation was also found for hydrogen, with the BP/OP medium presenting 8.30%, distinct from the BP/PP and BP/OP/PP media, which had concentrations of 7.04 and 7.54%, respectively. Nitrogen levels varied among all media ($P < 0.05$), with BP/PP exhibiting 5.98%, BP/OP 2.48%, and BP/OP/PP 3.41%. Sulfur content, however, did not show significant differences among the media, with measurements of 0.25, 0.28, and 0.36% for BP/PP, BP/OP, and BP/OP/PP, respectively (Figure 3B). These results of elemental quantification (CHNS) are consistent with values obtained in similar studies using waste-derived media for yeast cultivation.[69,81]

The substantial carbon and nitrogen contents detected across the media underscore the capacity of these agro-industrial residues to serve as nutrient-rich platforms for microbial growth. This not only supports the feasibility of using such waste streams in biotechnological applications but also prompts a closer examination of waste valorization strategies that can tap into the intrinsic nutrient composition of these residues for sustainable biomass production.[82]

3.5. Production of Bioplastics (EPS) from Banana, Potato, and Orange Peels. In recent decades, the production of bioplastics (EPS) has gained enormous interest in the scientific and industrial fields due to its biocompatible, biodegradable, and nontoxic characteristics.[83] These properties make EPS emulsifying and versatile, becoming a major alternative to chemical polymers derived from plants and algae.[84] EPS also possesses techno-functional properties with various applications (films, recombinant drugs, gelling agents, stabilizers, anti-inflammatory, and antimicrobial agents) in the pharmaceutical, medical, and food industries.[85−88] Therefore,

https://doi.org/10.1021/acsomega.4c05924
ACS Omega 2024, 9, 42970−42989

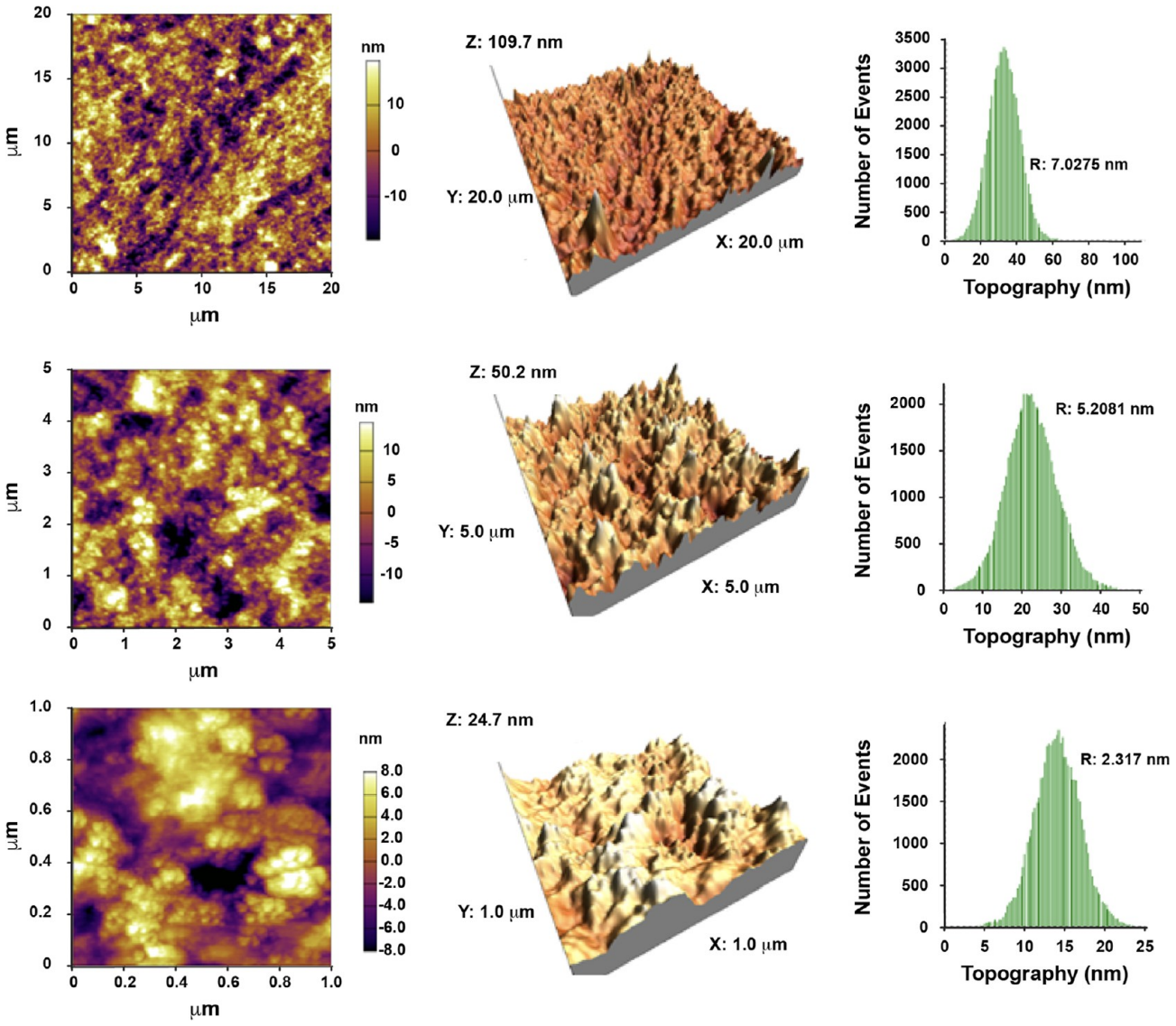

Figure 11. Morphology and AFM topographical distribution in 2D and 3D of the thin film of bioplastic OP.

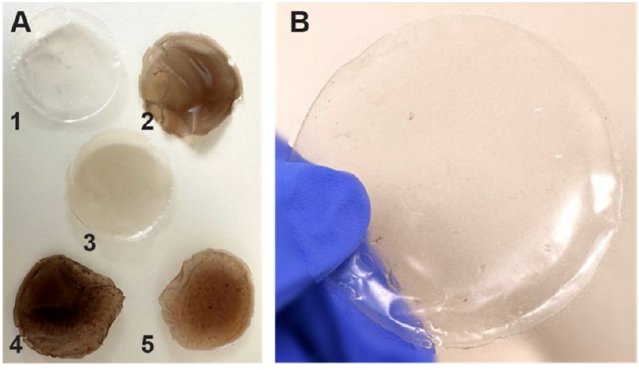

Figure 12. EPS films made from banana, potato, and orange peels. (A) 1) OP EPS film, 2) BP EPS film, 3) BP/OP EPS film, 4) BP/PP EPS film, and 5) BP/OP/PP EPS film. (B) Close-up to the OP EPS film.

microorganisms producing EPS and various sources of organic and commercial nutrients that allow higher EPS yield have been thoroughly studied.[89] In this case, we evaluated the feasibility of EPS production using banana, potato, and orange peels as nutrient sources for *R. mucilaginosa* UANL-001L. This study, in addition to being an innovative approach, contributed to the sustainable management of agro-industrial waste and opened the possibility of producing bioplastics with enormous potential in the industry.

The production of EPS from extracts based on banana, potato, orange peels, and their combinations, along with the YM medium, was evaluated in terms of mg/L after 96 h of incubation of the extracts with *R. mucilaginosa* UANL-001L. The results revealed significant differences in EPS production among all treatments, with a significance level of $P < 0.05$. The EPS production from the OP extract, with a value of 860.33 mg/L, was significantly higher ($P < 0.05$) compared to other evaluated extracts (Figure 4), highlighting the potential of OP to be used as a nutrient source for EPS synthesis mediated by *R. mucilaginosa* UANL-001L, even doubling the production of commercial YM (416.33 mg/L), which has the suitable composition for the optimal development of this yeast.[20,43,65]

The BP, PP, BP/PP, and BP/OP extracts, with EPS values of 391.43, 357.67, 469.40, and 382.50 mg/L, respectively, with no significant differences ($P > 0.05$), did not show variations compared to EPS production with YM. These results were

https://doi.org/10.1021/acsomega.4c05924
ACS Omega 2024, 9, 42970−42989

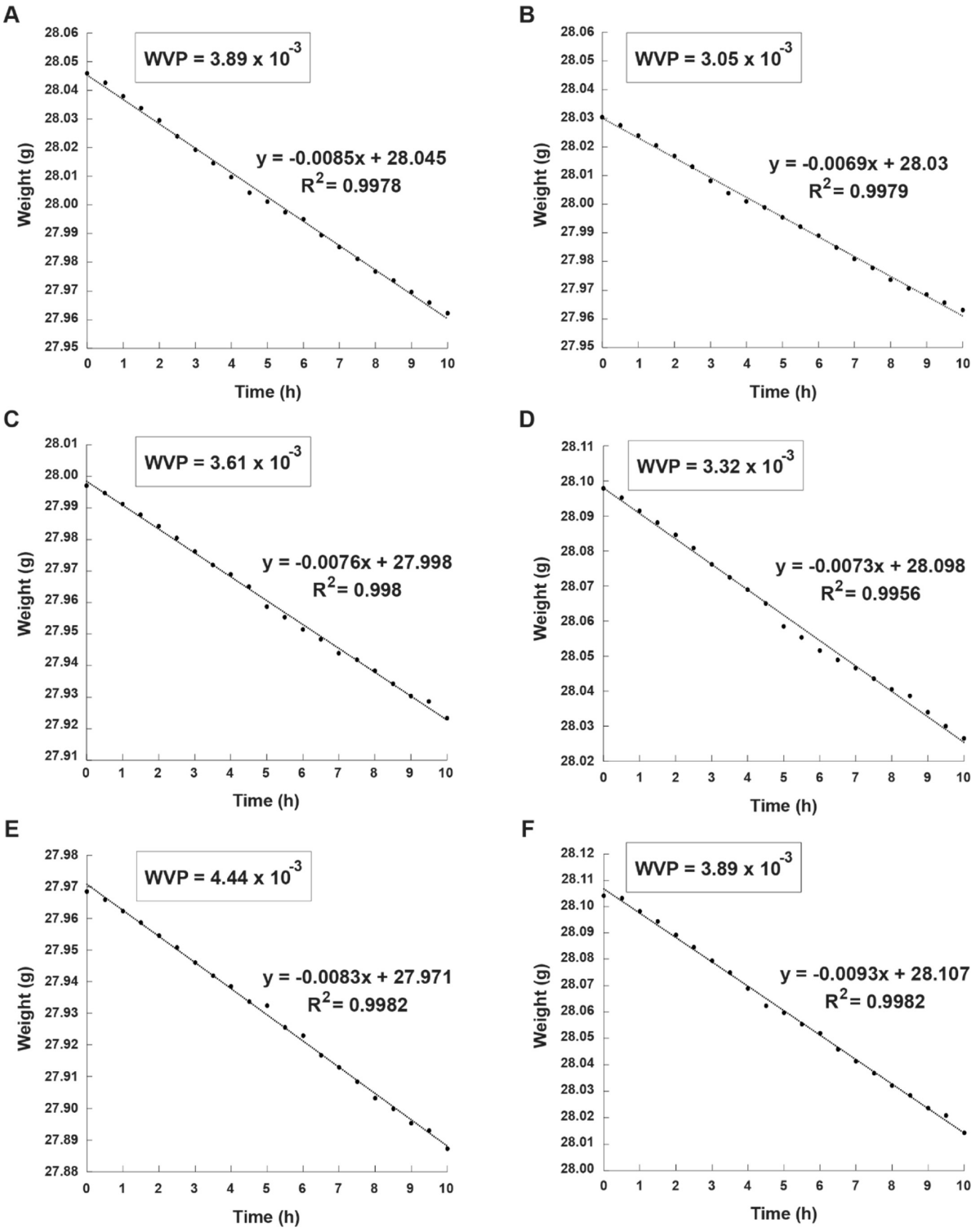

Figure 13. WVP results of EPS films: (A) BP films; (B) OP films; (C) PP films; (D) BP/OP films; (E) BP/PP films; and (F) BP/OP/PP films.

similar to values (417.4 and 404.5 mg/L) reported by Torres-Alvarez et al. (2022)[19] for EPS production using BP and YM as nutrient sources. Additionally, the BP/OP/PP extract recorded significantly lower EPS production than all other extracts, with a value of 272.67 mg/L, despite the high total solid content in the BP/OP/PP medium (Table 1), mainly derived from various mono- and polysaccharides in banana, potato, and orange peels.[90−92]

Based on the results obtained in terms of EPS production, the OP extract constitutes the most effective source, followed by BP and PP extracts, with the lowest value. Among the combined extracts, BP/OP is the most viable for EPS synthesis, followed by BP/PP, while the BP/OP/PP extract proved to be the least viable substrate for EPS production among the seven treatments evaluated, including the YM control medium. Differences in the results could be attributed to the unique chemical composition of each peel, such as

https://doi.org/10.1021/acsomega.4c05924
ACS Omega 2024, 9, 42970−42989

Table 3. Solubility Percentage of EPS Films in Water and Absolute Ethanol

	solubility of EPS films (%)	
films	water	ethanol absolute
BP	90.09	1.96
OP	64.71	1.05
PP	79.49	3.81
BP/OP	82.69	2.04
BP/PP	71.84	3.85
BP/OP/PP	73.40	3.42

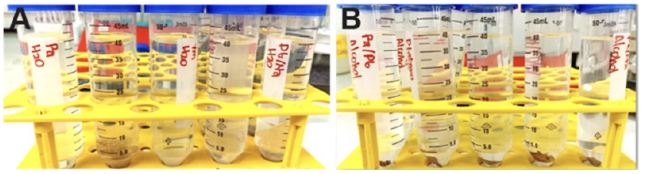

Figure 14. EPS films after 6 h of immersion in absolute ethanol: (A) immersion of the films in water and (B) immersion of the films in ethanol.

phenolic and flavonoid compounds, pectins, anthocyanins, pigments, antioxidants, oligosaccharides, cellobiose, fatty acids, proteinaceous and enzymatic compounds, among others, influencing the availability and assimilation of substrates by *R. mucilaginosa* for EPS synthesis.[1,93−97] Finally, these findings could positively influence sustainable production processes and the valorization of agro-food waste.

3.6. Chemical Characterization of EPS Using the FTIR Technique. Detailed information about the structure and chemical composition of EPS based on banana, orange, and potato peels was obtained through FTIR spectroscopy analysis, observing relevant functional groups. In Figure 5, the spectra of bioplastics from YM, BP, BP/PP, BP/OP, BP/OP/PP, PP, and OP are shown, all presenting similar peaks throughout the spectrum. The YM medium exhibited stretching at 3600−3200 cm^{-1} corresponding to the hydroxyl group (O−H), the peak at 2900 cm^{-1} for the methyl group (C−H), the band at 1650−1540 cm^{-1} for enol and amine groups, the carboxyl group (C═O) at 1350 cm^{-1}, stretching at 1250 $cm^{-1}$for the alkene (C═C), and finally, stretching at 1000−1200 cm^{-1} corresponding to the regions of C−O, C−C, C−O−C, and C−O−H groups, characteristic of an exopolysaccharide.[20,43,98]

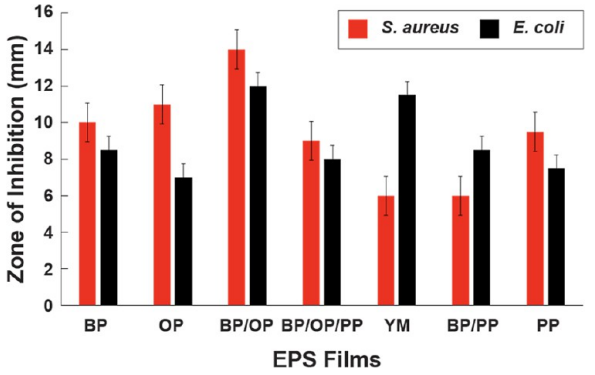

Figure 16. ZOI values of EPS films made from banana, orange, and potato peels against *S. aureus* and *E. coli*.

The BP extract in its spectrum recorded stretching regions at 3600−3000, 2924, 1734, 1637−1350, 1150−1000, and 1000−500 cm^{-1}, corresponding to the O−H, C−H, C═O, C═C, C−O−C, C−O−H, and Si−O functional groups (Figure 5). The presence of Si−O indicates that BP EPS, in addition to functional groups and aromatic rings typical of polysaccharides, also registered the presence of Si−O, a quality that could be conferred by the substrate, as BPs have a high content of metals such as K, Mg, Si, and others.[99−101]

As for the EPS from combined extracts BP/PP, BP/OP, and BP/OP/PP, consisting of 50% BP, their chemical composition showed the same functional groups and aromatic rings present in the BP extract but with a more pronounced expression of peaks, especially in the BP/OP/PP medium (Figure 5). The stretching regions recorded were 3700−3000 cm^{-1} (O−H), 2924 cm^{-1} (C−H), stretching of aromatic rings (C═O) at 1734 cm^{-1}, 1637−1350 cm^{-1} C−O−C, and C−O−H groups at 1150−1000 cm^{-1}, and finally, the silica band (Si−O) at 1000−500 cm^{-1}, as shown in Figure 5. These results were analogous to the findings of other authors regarding FTIR spectra resulting from the use of individual and combined banana, orange, and potato peels.[99,102−104]

The OP EPS presented stretching regions typical of a polysaccharide with less-pronounced bands in the 3650−3000 and 1900 cm^{-1} region (H−O and C−H), stretches in the 1637−1350 cm^{-1} region of aromatic compounds, and its most pronounced peak was in the 1150−1000 cm^{-1} region corresponding to vibrations of C−O−C and C−O−H groups

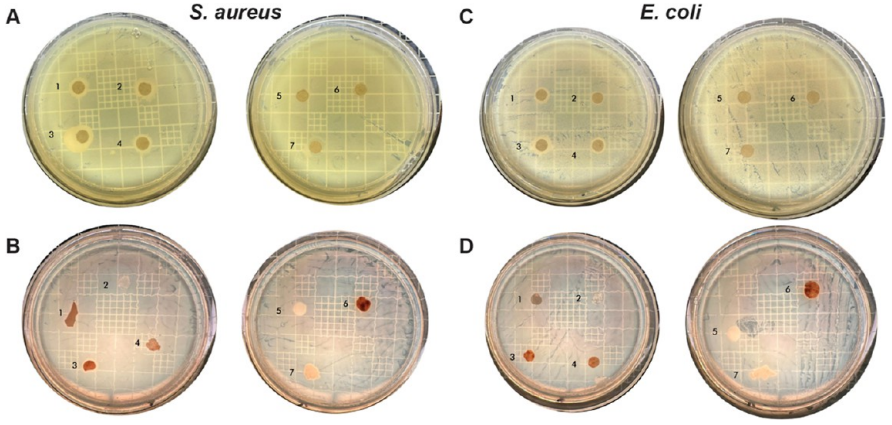

Figure 15. Bacterial ZOI of EPS films: (A) ZOI of *S. aureus* with the aqueous film; (B) ZOI of *E. coli* with the aqueous film; (C) ZOI of *S. aureus* with the dry film; and (D) ZOI of *E. coli* with the dry film.

https://doi.org/10.1021/acsomega.4c05924
ACS Omega 2024, 9, 42970−42989

(Figure 5). Meanwhile, PP EPS exhibited milder stretches than OP EPS in the O−H and C−H group region (3650−3000 and 1900 cm^{-1}), more pronounced peaks in the amino and carboxyl group area (1600−1250 cm^{-1}), and finally recorded the largest peak in the region of C−O−C and C−O−H groups, characteristic of this substrate. The resulting spectra of EPS from orange and potato peels showed characteristic bands of the chemical properties of mono- and polysaccharides specific to these residues, according to reports from other sources.[34,105−107]

3.7. Characterization of EPS Films. *3.7.1. Topographical Characterization of Films through AFM.* Bioplastic thin films were fabricated using BP, PP, and OP extracts by employing the spin-coating technique. AFM was utilized to meticulously characterize the surface morphology of these films, assessing parameters, such as thickness, roughness, and texture. Detailed surface topographical analysis was performed at varying scan sizes of 20 μm, 5 μm, and 1 μm, with resultant images presented in both two- and three-dimensional views across Figures 5−10.

The BP-derived film was subjected to nanoscale topographical analysis (Figure 6), revealing a rough surface characterized by irregular protrusions. Notably, the roughness values varied with scan size, achieving a maximum of 2.8545 nm at 5 μm and a minimum of 1.9936 nm at 20 μm. Such variability in roughness can be attributed to inconsistencies in sample preparation and the inherent properties of the substrate, which may lead to uneven distribution and agglomeration of particles.[108,109] Additionally, the presence of noncompact networks within the film could further enhance its roughness, potentially increasing its permeability—a characteristic important for certain applications.[110] Thickness measurements were consistently below 115 nm for all scans, with the thinnest layer measuring 31.1 nm at the 1 μm scan level (Figure 6). These findings are in line with other research on BP-based films, especially when used in combination with other biopolymers like chitosan, confirming the reproducibility and reliability of our fabrication process and its potential utility in sustainable material development.[111,112]

In the AFM examination of the composite bioplastic film derived from the combination of BP/OP, the images captured (Figure 7) demonstrate a significantly smoother and more homogeneous texture compared to that of the BP-only film. Notably, the roughness metrics varied with scanning scale; the roughest surface was measured at 0.5791 nm during the 5 μm scan, while the smoothest was recorded at 0.2067 nm in the 20 μm scan. The thickness of this composite film varied considerably, achieving its minimum at 6.5 nm in the 1 μm scan and its maximum at 31.7 nm in the 5 μm scan (Figure 7). The enhanced uniformity and reduced roughness of the BP/OP film suggest a more suitable interaction between the BP and OP extracts, which likely promotes more efficient spreadability and homogenization of the film matrix, thus resulting in a superior surface quality that could enhance adhesion properties in practical applications. Moreover, the low roughness allowed for a more uniform film with a high-quality interface, capable of better adherence to other surfaces.[110,113]

For the BP/PP and BP/OP/PP films, the AFM studies (Figures 8 and 9) depict a comparatively rougher topography with distinct surface reliefs that are more pronounced in the 5 and 20 μm scans. The finest texture was observed at the 1 μm scale, where the roughness and thickness were recorded at 2.9052 and 53.1 nm for BP/PP, and 2.7097 and 24.7 nm for BP/OP/PP, respectively. Such textural features suggest the presence of microscale agglomerates within the film matrix, potentially due to the complex interplay of different biopolymer constituents during the film formation process.[114] This hypothesis is supported by similar findings in the literature, where interactions among biopolymer components under varied processing conditions are known to affect the microstructure and thus the functional attributes of the resulting films.[109,113]

In our study, AFM was employed in noncontact mode to elucidate the surface topography of bioplastic films derived from PP, as depicted in Figure 10. Across three scanning resolutions (20, 5, and 1 μm), the film surface exhibited roughness measurements ranging from 4 to 5.5 nm, with the most refined surface texture observed at the 1 μm resolution, displaying roughness and thickness of 4.3159 and 48.5 nm, respectively. The AFM visualizations revealed an inherently irregular texture, characterized by the sporadic presence of protrusions and pores. Such topographical irregularities are inherent to organic substrates and reflect the microscale structural diversity that can influence the material properties. Previous research corroborates that organic materials frequently exhibit such microscale irregularities, which may not be perceptible at the macroscale but are crucial for applications requiring precise surface characteristics.[115] The AFM images of this film are identical to those reported by other authors; however, our roughness and thickness values are lower than those reported by these authors.[116,117]

Similarly, the OP film analyzed in Figure 11 demonstrated a range of roughness from 2.317 to 7.0275 nm across the different scan sizes (20, 5, and 1 μm), with the lowest value in the 1 μm scan and the highest in the 20 μm scan. This variance in roughness and thickness, which ranged from 24.7 nm at 1 μm to 109.7 nm at 20 μm, underscores the influence of scan resolution on perceived material properties and the importance of controlled processing conditions (Figure 11). The observed discrepancy in thickness and roughness might also be attributed to the absence of thermal treatment during the processing, which is known to facilitate more uniform dissolution of polysaccharides, thereby enhancing the homogeneity and surface smoothness of the resulting films.[113]

While our findings show lower roughness and thickness compared to similar studies, they align with the reported morphological characteristics of bioplastic surfaces, affirming the reproducibility and reliability of our methodological approach.[118,119]

The AFM analysis not only elucidates the microscale topographical characteristics of bioplastic films derived from banana, potato, and orange peels but also underscores the critical role of substrate composition and processing conditions in film properties. The observed variance in roughness and thickness across different films emphasizes the importance of substrate homogeneity and processing precision in achieving desirable film qualities. For instance, the higher roughness in the BP films might suggest a need for improved homogenization or a different approach to substrate preparation, such as finer grinding or a modified drying process, to enhance particle uniformity. Moreover, the comparative smoothness and uniformity in films involving OP may reflect a more favorable interaction of phytochemicals present in OPs with the bioplastic matrix, facilitating smoother film formation.

https://doi.org/10.1021/acsomega.4c05924
ACS Omega 2024, 9, 42970−42989

These topographical characteristics are pivotal not only for academic understanding but also for practical applications, such as in packaging, where smoothness and uniformity can affect material handling and barrier properties. The observed variations also highlight potential areas for further research in optimizing bioplastic formulations and processing parameters to tailor the surface properties to specific application needs. By leveraging the detailed insights provided by AFM analysis, future studies could focus on the manipulation of processing variables and the exploration of cross-linking agents or plasticizers that could enhance the structural and surface characteristics of bioplastics derived from agro-industrial wastes. Such advancements could significantly contribute to the development of sustainable packaging materials that are not only environmentally friendly but also functionally competitive with conventional plastics.

3.7.2. Water Vapor Permeability. Figure 12 displays images of the EPS films made from banana, potato, and orange peels before undergoing characterization. The results for WVP enabled the quantification of the amount of water diffusing per unit area through the EPS films.[120] All of the films exhibited consistent WVP trends and regression slopes, with determination coefficients exceeding 0.9950 ($R^2 > 0.9950$). The WVP values (g/m·s·Pa) recorded were as follows: 3.89×10^{-3} for the BP film, 3.05×10^{-3} for the OP film, 3.61×10^{-3} for the PP film, 3.32×10^{-3} for the BP/OP film, 4.44×10^{-3} for the BP/PP film, and 3.89×10^{-3} for the BP/OP/PP film. Notably, the BP and PP films shared the same WVP value, with the OP film displaying the lowest value and the BP/PP film displaying the highest. The WVP of all films was higher than the permeability values reported for polyethylene, chitosan, alginate, and pullulan films.[46,121−123] This variation in WVP may be attributed to the intrinsic nature of the compounds present in the films, as banana, potato, and orange peels contain polysaccharides with high hydrophilic properties and a relatively low water barrier compared to commercial polysaccharides and synthetic polymers.[91,95,124] The EPS matrix from banana, potato, and orange peels is characterized by a high content of hydroxyl and amino groups (Figure 5), which are capable of interacting with water molecules, thereby enhancing the water permeability across the film surfaces (see Figure 13).[107,125]

3.7.3. Solubility of EPS Films. The solubility data for all EPS films are presented in Table 3 and Figure 14A,B. All six evaluated films demonstrated water solubility values exceeding 60%, with the BP film being the most water-soluble, while the OP film exhibited the lowest solubility (Table 3). The ethanol solubility percentage for all of the films was below 4%, with the highest solubility values observed in the films containing PP in their composition (PP, BP/PP, and BP/OP/PP), whereas the OP film displayed the lowest ethanol solubility (Table 3). The water solubility results corroborate the WVP findings, indicating that all films possess an affinity for water molecules due to the hydrophilic nature of their constituents.[47] However, the low solubility in ethanol is encouraging as it suggests that these films may offer a substantial barrier to the permeability and evaporation of organic solvents. Furthermore, given their high WVP and low solubility in ethanol, these films present potential applications as coatings for fruits and vegetables, packaging for nonalcoholic beverages and products containing fats and oils, and as packaging materials for cleaning and pharmaceutical products that require moisture retention and are sensitive to ethanol (e.g., wet wipes, creams, lotions, among others).[8,122,124,126]

3.7.4. Antimicrobial Efficacy of EPS Films. Bacteriostatic tests using the ZOI method revealed that EPS films made from banana, potato, and orange peels exhibit antimicrobial activity against *S. aureus* and *E. coli* (ATCC). The ZOI was more diffuse and broader when evaluated using the filter method and aqueous solutions of the films against *S. aureus* and *E. coli* (Figure 15A,C). In contrast, no quantifiable inhibition halos were observed when the films were directly deposited on the agar surface. However, there was no bacterial growth on the surface of the films, which remained intact during the evaluation period (Figure 15B,D). The absence of halos can be attributed to the low moisture content of the films, which limited their rapid diffusion in the agar. Greater antimicrobial efficacy was observed against *S. aureus*, except for the YM and BP/PP films (Figure 16), which did not produce a noticeable halo. The OP and PP films displayed the smallest halos against *E. coli* (Figure 16). The combined BP/OP film demonstrated the highest antimicrobial efficacy compared with the other films against both bacteria tested (Figure 16). The antimicrobial activity of these films may be associated with their high content of hydroxyl, amino, and carbonyl groups (Figure 5), which facilitate the formation of hydrogen bonds with water molecules, reducing water availability and thus inhibiting microbial growth. Additionally, these functional groups have the capacity to interact with the microorganism's cell membrane, altering its integrity.[125−127]

4. CONCLUSIONS

This study has demonstrated the efficacy of utilizing BP, PP, and OP extracts as substrates for the production of bioplastics mediated by *R. mucilaginosa* UANL-001L. Notably, OP extracts exhibited particularly high potential, yielding bioplastics at double the rate compared to other substrates, including the commercially formulated YM medium optimized for the growth of this yeast strain. This suggests that OP extracts may contain unique components that enhance the bioplastic synthesis, highlighting their potential for industrial applications.

All of the bioplastics generated in this study were successfully converted into thin films with high-quality morphological properties. The roughness of each film consistently remained below 8 nm, indicating strong interfacial compatibility and cohesiveness within the bioplastic matrix. Particularly noteworthy were the films derived from the combination of BP and OP (BP/OP), which exhibited the most interesting morphological characteristics, including the lowest measured thickness and a highly uniform, compact, and subtly smooth texture. Additionally, this film demonstrated superior antimicrobial efficacy (ZOI) against both Gram-positive and Gram-negative bacteria. Conversely, the single OP film reported the best WVP and solubility in water and ethanol compared to those of the other films.

Looking forward, these findings suggest the need for further investigation into the conversion of agro-industrial waste, particularly OP, into bioplastics with optimized potential applications. Further research should aim to optimize the biochemical pathways involved. Additionally, the remarkable properties of all of the films, especially OP and BP/OP, suggest a potential for developing advanced bioplastic materials with high-value physicochemical attributes. Such materials could find significant applications in environmentally sustainable

https://doi.org/10.1021/acsomega.4c05924
ACS Omega 2024, 9, 42970−42989

packaging and other sectors in which high-quality biodegradable films are crucial. Exploring the scalability of these bioplastics in industrial applications will be essential to meeting the urgent global demand for sustainable alternatives to conventional plastics.

■ ASSOCIATED CONTENT

Data Availability Statement

All data generated or analyzed during this study are included in this published article.

■ AUTHOR INFORMATION

Corresponding Author

José Rubén Morones-Ramírez − *Faculty of Chemical Sciences, Autonomous University of Nuevo León (UANL), San Nicolás de los Garza 66455, Mexico; Center for Research in Biotechnology and Nanotechnology, Faculty of Chemical Sciences, Autonomous University of Nuevo León, Research and Technological Innovation Park, Apodaca 66628, Mexico;* orcid.org/0000-0001-7009-686X; Email: jose.moronesrmr@uanl.edu.mx

Authors

Diana Lucinda Castillo-Patiño − *Faculty of Chemical Sciences, Autonomous University of Nuevo León (UANL), San Nicolás de los Garza 66455, Mexico; Center for Research in Biotechnology and Nanotechnology, Faculty of Chemical Sciences, Autonomous University of Nuevo León, Research and Technological Innovation Park, Apodaca 66628, Mexico*

Humberto Geovani Rosas-Mejía − *Faculty of Chemical Sciences, Autonomous University of Nuevo León (UANL), San Nicolás de los Garza 66455, Mexico; Center for Research in Biotechnology and Nanotechnology, Faculty of Chemical Sciences, Autonomous University of Nuevo León, Research and Technological Innovation Park, Apodaca 66628, Mexico*

Alonso Albalate-Ramírez − *Faculty of Chemical Sciences, Autonomous University of Nuevo León (UANL), San Nicolás de los Garza 66455, Mexico; Center for Research in Biotechnology and Nanotechnology, Faculty of Chemical Sciences, Autonomous University of Nuevo León, Research and Technological Innovation Park, Apodaca 66628, Mexico*

Pasiano Rivas-García − *Faculty of Chemical Sciences, Autonomous University of Nuevo León (UANL), San Nicolás de los Garza 66455, Mexico; Center for Research in Biotechnology and Nanotechnology, Faculty of Chemical Sciences, Autonomous University of Nuevo León, Research and Technological Innovation Park, Apodaca 66628, Mexico*

Amanda Carrillo-Castillo − *Autonomous University of Ciudad Juarez, Ciudad Juárez 32310 Chihuahua, Mexico;* orcid.org/0000-0002-2787-2023

Complete contact information is available at: https://pubs.acs.org/10.1021/acsomega.4c05924

Author Contributions

Conceptualization, Diana Lucinda Castillo-Patiño and José Rubén Morones-Ramírez; writing—original draft preparation—Diana Lucinda Castillo-Patiño, Humberto Geovani Rosas-Mejía, and José Rubén Morones-Ramírez; writing—review and editing—Diana Lucinda Castillo-Patiño, Humberto Geovani Rosas-Mejía, Alonso Albalate-Ramírez, Pasiano Rivas-García, Amanda Carrillo-Castillo, and José Rubén Morones-Ramírez. All authors have read and agreed to the published version of the manuscript.

Funding

The authors want to thank the Universidad Autonoma de Nuevo León and CONAHCyT for providing financial support through Paicyt 2019−2020, Paicyt 2020−2021, and Paicyt 2022−2023 Science Grants. CONAHCyT grants for: Basic science grant 221332, Fronteras de la Ciencia grant 1502, Infraestructura grant 279957, and Apoyos a la Ciencia de Frontera grant 316869 y grant a Ciencia de Frontera CF-2023-I-1327. In addition, we would like to thank CTR for their funding support toward the development of this research project. Diana Lucinda Castillo-Patiño, Humberto Geovani Rosas-Mejía, and Alonso Albalate-Ramírez thank the support from Beca Nacional de Posgrado from CONACyT.

Notes

The authors declare no competing financial interest.

■ REFERENCES

(1) El Barnossi, A.; Housseini, A. I. Physico-chemical characterization of decomposing banana, pomegranate and mandarin peels in water and soil for a sustainable valorization. *Ind. Crops Prod.* **2023**, *193*, 116207.

(2) Cury R, K.; Aguas, M.; Yelitza, M. M.; Esp, A.; Olivero V, R.; Rafael, C. C. L. Residuos agroindustriales su impacto, manejo y aprovechamiento. *Rev. Colombiana Cienc. Anim.* **2017**, *9*, 122−132.

(3) Vargas Corredor, Y. A.; y Peréz Pérez, L. I. *Aprovechamiento de residuos agroindustriales en el mejoramiento de la calidad del ambiente*; Revista Facultad de Ciencias Básicas, 2018; pp 59−72.

(4) Melnichuk, N.; Braia, M. J.; Anselmi, P. A.; Meini, M. R.; Romanini, D. Valorization of two agroindustrial wastes to produce alpha-amylase enzyme from Aspergillus oryzae by solid-state fermentation. *Waste Manage.* **2020**, *106*, 155−161.

(5) Kraśniewska, K.; Gniewosz, M.; Synowiec, A.; Przybył, J. L.; Bączek, K.; Węglarz, Z. The use of pullulan coating enriched with plant extracts from Satureja hortensis L. to maintain pepper and apple quality and safety. *Postharvest Biol. Technol.* **2014**, *90*, 63−72.

(6) Ng, H. S.; Kee, P. E.; Yim, H. S.; Chen, P. T.; Wei, Y. H.; Chi-Wei Lan, J. Recent advances on the sustainable approaches for conversion and reutilization of food wastes to valuable bioproducts. *Bioresour. Technol.* **2020**, *302*, 122889.

(7) Adimas, M. A.; Abera, B. D. Valorization of fruit and vegetable by-products for extraction of pectin and its hydrocolloidal role in low-fat yoghurt processing. *LWT* **2023**, *189*, 115534.

(8) Silva-Weiss, A.; Bifani, V.; Ihl, M.; Sobral, P. J. A.; Gómez-Guillén, M. Polyphenol-rich extract from murta leaves on rheological properties of film-forming solutions based on different hydrocolloid blends. *J. Food Eng.* **2014**, *140*, 28−38.

(9) Jhon Enrique, Z. Z.; Alex Alberto, D.-R.; Aixa Rosa, G. V. Biomass Of Agricultural Waste For Agroindustrial Products Obtaining: Potentialities And Challenges In Ecuador. *Cent. Azúcar* **2021**, *52* (48), 120−133.

(10) Salinas, L. F. M.; Gallo-Castro, F. J.; Zuluaga-Huertas, J. P. Aprovechaniento de Residuos de Cáscara de Cítricos en la Concepción de Vajillas Biodegradables. *Encuentro Internacional Educación Ingeniería-ACOFI* **2021**, *8*, 1−10.

(11) Mada, T.; Duraisamy, R.; Guesh, F. Optimization and characterization of pectin extracted from banana and papaya mixed peels using response surface methodology. *Food Sci. Nutr.* **2022**, *10*, 1222−1238.

(12) Morocho, M. T.; Leiva-mora, M. Microorganismos efcientes, propiedades funcionales y aplicaciones agrícolas. *Cent. Agric.* **2019**, *46*, 93−103.

(13) Rojas-gonzález, A.; Flores-Montes, C.; López-Rodríguez, D. Use prospects of some agroindustrial waste Introducción. *Revista Cubana de Química* **2019**, *46*, 21.

https://doi.org/10.1021/acsomega.4c05924
ACS Omega 2024, 9, 42970−42989

(14) Sarria, S.; Kruyer, N. S.; Peralta-Yahya, P. Microbial synthesis of medium-chain chemicals from renewables. *Nat. Biotechnol.* **2017**, *35*, 1158−1166.
(15) Ayadi, I.; Belghith, H.; Gargouri, A.; Guerfali, M. Utilization of Wheat Bran Acid Hydrolysate by Rhodotorula mucilaginosa Y-MG1 for Microbial Lipid Production as Feedstock for Biodiesel Synthesis. *Biomed. Res. Int.* **2019**, *2019*, 1−11.
(16) Ghilardi, C.; Sanmartin Negrete, P.; Carelli, A. A.; Borroni, V. Evaluation of olive mill waste as substrate for carotenoid production by Rhodotorula mucilaginosa. *Bioresour. Bioprocess.* **2020**, *7*, 52.
(17) Ramos, A.; Cabero, M.; Orden, B.; Ángel-moreno, A.; Forés, R. Fungemia por Rhodotorula mucilaginosa. Presentación de dos casos. *Rev. Esp Quimioter* **2012**, *25*, 76−78.
(18) Medina-Ramirez, C. F.; Castañeda-Guel, M. T.; Alvarez-Gonzalez, M. F.; Montesinos-Castellanos, A.; Morones-Ramirez, J. R.; López-Guajardo, E. A.; Gómez-Loredo, A. Application of Extractive Fermentation on the Recuperation of Exopolysaccharide from Rhodotorula mucilaginosa UANL-001L. *Fermentation* **2020**, *6*, 108.
(19) Torres-Alvarez, D.; León-Buitimea, A.; Albalate-Ramírez, A.; Rivas-García, P.; Hernández-Núñez, E.; Morones-Ramírez, J. R. Conversion of banana peel into diverse valuable metabolites using an autochthonous Rhodotorula mucilaginosa strain. *Microb. Cell Factories* **2022**, *21*, 96.
(20) Vazquez-Rodriguez, A.; Vasto-Anzaldo, X. G.; Barboza Perez, D.; Vázquez-Garza, E.; Chapoy-Villanueva, H.; García-Rivas, G.; Garza-Cervantes, J. A.; Gómez-Lugo, J. J.; Gomez-Loredo, A. E.; Garza Gonzalez, M. T.; et al. Microbial Competition of Rhodotorula mucilaginosa UANL-001L and E. coli increase biosynthesis of Non-Toxic Exopolysaccharide with Applications as a Wide-Spectrum Antimicrobial. *Sci. Rep.* **2018**, *8*, 798.
(21) Ali, A.; Chen, Y.; Liu, H.; Yu, L.; Baloch, Z.; Khalid, S.; Zhu, J.; Chen, L. Starch-based antimicrobial films functionalized by pomegranate peel. *Int. J. Biol. Macromol.* **2019**, *129*, 1120−1126.
(22) Hanani, Z. N.; Yee, F. C.; Nor-Khaizura, M. A. R. Effect of pomegranate (Punica granatum L.) peel powder on the antioxidant and antimicrobial properties of fish gelatin films as active packaging. *Food Hydrocolloids* **2019**, *89*, 253−259.
(23) Karakuş, E.; Ayhan, Z.; Haskaraca, G. Development and characterization of sustainable-active-edible-bio based films from orange and pomegranate peel waste for food packaging: Effects of particle size and acid/plasticizer concentrations. *Food Packag. Shelf Life* **2023**, *37*, 101092.
(24) Varghese, R.; Vijay, V. S.; Unnikrishnan, G.; Megha, M.; Swaminathan, R.; Thomas, J.; Senthilkumar, M.; Ayyasamy, S. Lithium trivanadate thin films by polymer-assisted spin coating method for supercapacitor applications. *Micro Nanostruct.* **2023**, *180*, 207606.
(25) Eça, K. S.; Sartori, T.; Menegalli, F. C. Films and edible coatings containing antioxidants - a review. *Braz. J. Food Technol.* **2014**, *17*, 98−112.
(26) Na, J. Y.; Kang, B.; Sin, D. H.; Cho, K.; Park, Y. D. Understanding Solidification of Polythiophene Thin Films during Spin-Coating: Effects of Spin-Coating Time and Processing Additives. *Sci. Rep.* **2015**, *5*, 13288.
(27) Nisticò, R.; Scalarone, D.; Magnacca, G. Sol-gel chemistry, templating and spin-coating deposition: A combined approach to control in a simple way the porosity of inorganic thin films/coatings. *Microporous Mesoporous Mater.* **2017**, *248*, 18−29.
(28) Samal, S.; Kosjakova, O. Surface feature of PMMA films on NiTi alloy substrate by the spin coating method. *Ceram. Int.* **2023**, *49*, 24370−24378.
(29) McClements, J.; Zhang, M.; Radacsi, N.; Koutsos, V. Measuring the interactions between carbon black nanoparticles and latex thin films in aqueous media using AFM force spectroscopy. *Colloids Surf. A Physicochem Eng. Asp* **2020**, *603*, 124920.
(30) Mwema, F. M.; Akinlabi, E. T.; Oladijo, O. P. Dependence of fractal characteristics on the scan size of atomic force microscopy (AFM) phase imaging of aluminum thin films. *Mater. Today Proc.* **2020**, *26*, 1540−1545.
(31) Roa, S.; Sirena, M.; Morán, M. Stress-induced pseudoelasticity in freestanding Cu−Al−Ni thin film by AFM-assisted nano-indentation. *Solid State Commun.* **2023**, *361*, 115071.
(32) Wu, Y.; Zhang, Y.; Jiang, Y.; Qian, Y.; Guo, X.; Wang, L.; Zhang, J. Orange peel extracts as biodegradable corrosion inhibitor for magnesium alloy in NaCl solution: Experimental and theoretical studies. *J. Taiwan Inst Chem. Eng.* **2020**, *115*, 35−46.
(33) Javed, A.; Ahmad, A.; Ali, T.; Umair, S.; Muhammad, N. Potato peel waste-its nutraceutical, industrial and biotechnological applacations. *AIMS Agriculture and Food* **2019**, *4*, 807−832.
(34) Rehman, R.; Mahmud, T.; Irum, M. Comparative sorption studies for Amaranth dye removal from water in cost-effective way using Guava leaves and potato peels. *Asian J. Chem.* **2015**, *27*, 2008−2014.
(35) Suri, S.; Singh, A.; Nema, P. K. Current applications of citrus fruit processing waste: A scientific outlook. *Appl. Food Res.* **2022**, *2*, 1−16.
(36) Zhang, J.; Zhang, L.; Lai, C.; Liang, Y.; Gao, L.; Kaliaperumal, K.; Jiang, Y. Nutraceutical potential of navel orange peel in diabetes management: The chemical profile, antioxidant, α-glucosidase inhibitory and antiglycation effects of its flavonoids. *Food Biosci.* **2022**, *49*, 101943.
(37) Xia, J.; Shu, J.; Yao, K.; Xu, J.; Yu, X.; Xue, X.; Ma, D.; Lin, X. Synergism of cellulase, pectinase and xylanase on hydrolyzing differently pretreated sweet potato residues. *Prep. Biochem. Biotechnol.* **2020**, *50*, 181−190.
(38) Norma Mexicana & NMX-AA-034-SCFI-2015. *Secretaría De Economía Water Analisys-Measurement Of Salts And Solids Dissolved In Natural Water, Wastewaters And Treated Wastewaters-Test Method*, 2015.
(39) Sinkiewicz, I.; Śliwińska, A.; Staroszczyk, H.; Kołodziejska, I. Alternative methods of preparation of soluble keratin from chicken feathers. *Waste Biomass Valorization* **2017**, *8*, 1043−1048.
(40) Florida-Rofner, N.; Reategui-Diaz, F. Compost based on feathers of chickens (gallus gallus domesticus). *Livest. Res. Rural Dev.* **2019**, *31*, 1−10.
(41) Du, R.; Guo, W.; Shen, Y.; Dai, J.; Zhang, H.; Fu, M.; Wang, X. In situ assay of the reducing sugars in hydrophilic natural deep eutectic solvents by a modified DNS method. *J. Mol. Liq.* **2023**, *385*, 122286.
(42) Montañez, L. J. B. Cuantificación de azúcares reductores del sustrato en residuos de piña con el método del ácido 3,5-dinitrosalicílico. *Rev. Invest* **2020**, *13*, 57−66.
(43) Garza-Cervantes, J. A.; Escárcega-González, C. E.; Díaz Barriga Castro, E.; Mendiola-Garza, G.; Marichal-Cancino, B. A.; López-Vázquez, M. A.; Morones-Ramirez, J. R. mucilaginosa. *Int. J. Nanomed.* **2019**, *14*, 2557−2571.
(44) Filip, A. V.; Trefilov, A. M. I.; Boroica, L.; Dinca, M. C.; Elisa, M.; Vasiliu, I. C.; Tigau, N.; Brajnicov, S.; Dumitru, M.; Luculescu, C.; et al. Graphene oxide- boro-phosphate glass nano-composite thin films synthesized by sol-gel spin coating method. *J. Non-Cryst. Solids* **2023**, *613*, 122372.
(45) Dixit, A.; Sabnis, A.; Shetty, A. Antimicrobial Edible Films and Coatings based on N,O-Carboxymethyl Chitosan incorporated with Ferula Asafoetida (Hing) and Adhatoda Vasica (Adulsa) extract. *Adv. Mater. Process. Technol.* **2022**, *8*, 2699−2715.
(46) Cazón, P.; Morales-Sanchez, E.; Velazquez, G.; Vázquez, M. Measurement of the Water Vapor Permeability of Chitosan Films: A Laboratory Experiment on Food Packaging Materials. *J. Chem. Educ.* **2022**, *99*, 2403−2408.
(47) Marichelvam, M. K.; Jawaid, M.; Asim, M. Corn and Rice Starch-Based Bio-Plastics as Alternative Packaging Materials. *Fibers* **2019**, *7*, 32.
(48) Vaidya, M. Y.; McBain, A. J.; Butler, J. A.; Banks, C. E.; Whitehead, K. A. Antimicrobial Efficacy and Synergy of Metal Ions against Enterococcus faecium, Klebsiella pneumoniae and Acinetobacter baumannii in Planktonic and Biofilm Phenotypes. *Sci. Rep.* **2017**, *7*, 5911.

https://doi.org/10.1021/acsomega.4c05924
ACS Omega 2024, 9, 42970−42989

(49) Gonzalez Garza, M. T.; Barboza Perez, D.; Vazquez Rodriguez, A.; Garcia-Gutierrez, D. I.; Zarate, X.; Cantú Cardenas, M. E.; Urraca-Botello, L. I.; Lopez-Chuken, U. J.; Trevino-Torres, A. L.; Cerino-Córdoba, F. d. J.; et al. Metal-Induced Production of a Novel Bioadsorbent Exopolysaccharide in a Native Rhodotorula mucilaginosa from the Mexican Northeastern Region. *PLoS One* **2016**, *11*, No. e0148430.
(50) Vazquez-Rodriguez, A.; Vasto-Anzaldo, X. G.; Leon-Buitimea, A.; Zarate, X.; Morones-Ramirez, J. R. Antibacterial and antibiofilm activity of biosynthesized silver nanoparticles coated with exopolysaccharides obtained from Rhodotorula mucilaginosa. *IEEE Trans. NanoBioscience* **2020**, *19*, 498−503.
(51) Koochi, Z. H.; Jahromi, K. G.; Kavoosi, G.; Ramezanian, A. Fortification of Chlorella vulgaris with citrus peel amino acid for improvement biomass and protein quality. *Biotechnol. Rep.* **2023**, *39*, No. e00806.
(52) Lavanya, K. M.; Florence, J. A. K.; Vivekanandan, B.; Lakshmipathy, R. Comparative investigations of raw and alkali metal free banana peel as adsorbent for the removal of Hg2+ ions. *Mater. Today Proc.* **2022**, *55*, 321−326.
(53) Mohamed, R. M.; Hashim, N.; Abdullah, S.; Abdullah, N.; Mohamed, A.; Asshaary Daud, M. A.; Aidil Muzakkar, K. F. Adsorption of Heavy Metals on Banana Peel Bioadsorbent. *J. Phys.* **2020**, *1532*, 012014.
(54) Santos, C. M.; Dweck, J.; Viotto, R. S.; Rosa, A. H.; de Morais, L. C. Application of orange peel waste in the production of solid biofuels and biosorbents. *Bioresour. Technol.* **2015**, *196*, 469−479.
(55) Bhurat, K. S.; Banerjee, T.; Pandey, J. K.; Bhurat, S. S. A lab fermenter level study on anaerobic hydrogen fermentation using potato peel waste: effect of pH, temperature, and substrate pretreatment. *J. Mater. Cycles Waste Manag.* **2021**, *23*, 1617−1625.
(56) Carota, E.; Petruccioli, M.; D'Annibale, A.; Gallo, A. M.; Crognale, S. Orange peel waste−based liquid medium for biodiesel production by oleaginous yeasts. *Appl. Microbiol. Biotechnol.* **2020**, *104*, 4617−4628.
(57) Teshome, Z. T. Effects of banana peel compost rates on Swiss chard growth performance and yield in Shirka district, Oromia, Ethiopia. *Heliyon* **2022**, *8*, No. e10097.
(58) Tsado, A. N.; Okoli, N. R.; Jiya, A. G.; Gana, D.; Saidu, B.; Zubairu, R.; Salihu, I. Z. Proximate, minerals, and amino acid compositions of banana and plantain peels. *BIOMED Nat. Appl. Sci.* **2021**, *1* (1), 32−42.
(59) Carneiro, R. B.; Gomes, G. M.; Sabatini, C. A.; Gago-Ferrero, P.; Zaiat, M.; Santos-Neto, Á. J. Enhancing Organic Micropollutants Removal in Wastewater with an Innovative Two-Stage Anaerobic Fixed-Film Bioreactor: Role of Acidogenic and Methanogenic Steps. *ACS ES&T Eng.* **2024**, *4*, 354−364.
(60) Qin, D.; Dong, J. Multi-Level Optimization and Strategies in Microbial Biotransformation of Nature Products. *Molecules* **2023**, *28*, 2619.
(61) Calderón Celis, F.; González-Álvarez, I.; Fabjanowicz, M.; Godin, S.; Ouerdane, L.; Lauga, B.; Łobiński, R. Unveiling the Pool of Metallophores in Native Environments and Correlation with Their Potential Producers. *Environ. Sci. Technol.* **2023**, *57*, 17302−17311.
(62) Muiruri, J. K.; Yeo, J. C. C.; Zhu, Q.; Ye, E.; Loh, X. J.; Li, Z. Poly(hydroxyalkanoates): Production, Applications and End-of-Life Strategies-Life Cycle Assessment Nexus. *ACS Sustain. Chem. Eng.* **2022**, *10*, 3387−3406.
(63) Chaturvedi, S.; Kumari, A.; Bhatacharya, A.; Sharma, A.; Nain, L.; Khare, S. K. Banana peel waste management for single-cell oil production. *Energy, Ecol. Environ.* **2018**, *3*, 296−303.
(64) Machado, W. R. C.; Murari, C. S.; Duarte, A. L. F.; Del Bianchi, V. L. Optimization of agro-industrial coproducts (molasses and cassava wastewater) for the simultaneous production of lipids and carotenoids by Rhodotorula mucilaginosa. *Biocatal. Agric. Biotechnol.* **2022**, *42*, 102342.
(65) Escárcega-González, C. E.; Garza-Cervantes, J. A.; Vázquez-Rodríguez, A.; Morones-Ramírez, J. R. Bacterial exopolysaccharides as reducing and/or stabilizing agents during synthesis of metal nanoparticles with biomedical applications. *Int. J. Polym. Sci.* **2018**, *2018*, 7045852.
(66) Martins, L. C.; Palma, M.; Angelov, A.; Nevoigt, E.; Liebl, W.; Sá-Correia, I. Complete Utilization of the Major Carbon Sources Present in Sugar Beet Pulp Hydrolysates by the Oleaginous Red Yeasts Rhodotorula toruloides and R. mucilaginosa. *J. Fungi* **2021**, *7*, 215.
(67) Rodrigues, T. V. D.; Amore, T. D.; Teixeira, E. C.; Burkert, J. F. d. M. Carotenoid Production by Rhodotorula mucilaginosa in Batch and Fed-Batch Fermentation Using Agroindustrial Byproducts. *Food Technol. Biotechnol.* **2019**, *57*, 388−398.
(68) Da Silva, J.; Honorato da Silva, F. L.; Santos Ribeiro, J. E.; Nóbrega de Melo, D. J.; Santos, F. A.; Lucena de Medeiros, L. Effect of supplementation, temperature and pH on carotenoids and lipids production by Rhodotorula mucilaginosa on sisal bagasse hydrolyzate. *Biocatal. Agric. Biotechnol.* **2020**, *30*, 101847.
(69) Prabhu, A. A.; Gadela, R.; Bharali, B.; Deshavath, N. N.; Dasu, V. V. Development of high biomass and lipid yielding medium for newly isolated Rhodotorula mucilaginosa. *Fuel* **2019**, *239*, 874−885.
(70) Ayala, J. R.; Montero, G.; Coronado, M. A.; García, C.; Curiel-Alvarez, M. A.; León, J. A.; Sagaste, C. A.; Montes, D. G. Characterization of Orange Peel Waste and Valorization to Obtain Reducing Sugars. *Molecules* **2021**, *26*, 1348.
(71) El Kantar, S.; Boussetta, N.; Rajha, H. N.; Maroun, R. G.; Louka, N.; Vorobiev, E. High voltage electrical discharges combined with enzymatic hydrolysis for extraction of polyphenols and fermentable sugars from orange peels. *Food Res. Int.* **2018**, *107*, 755−762.
(72) Kumar, V. B.; Pulidindi, I. N.; Gedanken, A. Glucose production from potato peel waste under microwave irradiation. *J. Mol. Catal. Chem.* **2016**, *417*, 163−167.
(73) Martínez-Trujillo, M. A.; Bautista-Rangel, K.; García-Rivero, M.; Martínez-Estrada, A.; Cruz-Díaz, M. R. Enzymatic saccharification of banana peel and sequential fermentation of the reducing sugars to produce lactic acid. *Bioprocess Biosyst. Eng.* **2020**, *43*, 413−427.
(74) Palacios, S.; Ruiz, H. A.; Ramos-Gonzalez, R.; Martínez, J.; Segura, E.; Aguilar, M.; Aguilera, A.; Michelena, G.; Aguilar, C.; Ilyina, A. Comparison of physicochemical pretreatments of banana peels for bioethanol production. *Food Sci. Biotechnol.* **2017**, *26*, 993−1001.
(75) Nunes, J. M.; Bizerra, F. C.; Ferreira, R. C. e.; Colombo, A. L. Molecular identification, antifungal susceptibility profile, and biofilm formation of clinical and environmental Rhodotorula species isolates. *Antimicrob. Agents Chemother.* **2013**, *57*, 382−389.
(76) Grellet-Bournonville, C. F.; Di Peto, P. d. l. Á.; Cerviño Dowling, A. M.; Castagnaro, A. P.; Schmeda-Hirschmann, G.; Díaz Ricci, J. C.; Mamaní, A. I.; Filippone, M. P. Seasonal Variation of Plant Defense Inductor Ellagitannins in Strawberry Leaves under Field Conditions for Phytosanitary Technological Applications. *J. Agric. Food Chem.* **2021**, *69*, 12424−12432.
(77) Qiu, X.; Zhang, J.; Zhou, J.; Fang, Z.; Zhu, Z.; Li, J.; Du, G. Stress tolerance phenotype of industrial yeast: industrial cases, cellular changes, and improvement strategies. *Appl. Microbiol. Biotechnol.* **2019**, *103*, 6449−6462.
(78) Pereira, G. A.; Arruda, H. S.; Molina, G.; Pastore, G. M. Extraction optimization and profile analysis of oligosaccharides in banana pulp and peel. *J. Food Process Preserv.* **2018**, *42*, No. e13408.
(79) Witczak, T.; Witczak, M.; Stępień, A.; Bednarz, A.; Grzesik, M. State diagrams of candied orange peel obtained using different hypertonic solutions. *J. Food Eng.* **2017**, *212*, 234−241.
(80) Yu, Y.; Shi, S. Development and Perspective of Rhodotorula toruloides as an Efficient Cell Factory. *J. Agric. Food Chem.* **2023**, *71*, 1802−1819.
(81) Banerjee, A.; Vithusha, T.; Krishna, B. B.; Kumar, J.; Bhaskar, T.; Ghosh, D. Pyrolysis of de-oiled yeast biomass of Rhodotorula mucilaginosa IIPL32: Kinetics and thermodynamic parameters using thermogravimetric analysis. *Bioresour. Technol.* **2021**, *340*, 125534.
(82) Lui, M. Y.; Wong, C. Y. Y.; Choi, A. W. T.; Mui, Y. F.; Qi, L.; Horváth, I. T. Valorization of Carbohydrates of Agricultural Residues

https://doi.org/10.1021/acsomega.4c05924
ACS Omega 2024, 9, 42970−42989

and Food Wastes: A Key Strategy for Carbon Conservation. *ACS Sustain. Chem. Eng.* **2019**, *7*, 17799−17807.
(83) Sardari, R. R.; Kulcinskaja, E.; Ron, E. Y.; Björnsdóttir, S.; Karlsson, E. N. Evaluation of the production of exopolysaccharides by two strains of the thermophilic bacterium Rhodothermus marinus. *Carbohydr. Polym.* **2017**, *156*, 1−8.
(84) Fuentes, A. ·.; Carreño, C.; Llanos, C. Rendimiento de exopolisacáridos emulgentes producidos por bacterias halófilas nativas en tres concentraciones de melaza de Saccharum officinarum L. " caña de azúcar " Yield emulsifiers exopolysaccharides produced by native halophilic. *Sci. Agropecu.* **2013**, *4*, 111−120.
(85) Li, W.; Ji, J.; Rui, X.; Yu, J.; Tang, W.; Chen, X.; Jiang, M.; Dong, M. Production of exopolysaccharides by Lactobacillus helveticus MB2-1 and its functional characteristics in vitro. *LWT−Food Sci. Technol.* **2014**, *59*, 732−739.
(86) Moradi, M.; Guimaraes, J.; Sahin, S. Current applications of exopolysaccharides from lactic acid bacteria in the development of food active edible packaging. *Curr. Opin. Food Sci.* **2021**, *40*, 33−39.
(87) Tiwari, S.; Kavitake, D.; Devi, P. B.; Halady Shetty, P. Bacterial exopolysaccharides for improvement of technological, functional and rheological properties of yoghurt. *Int. J. Biol. Macromol.* **2021**, *183*, 1585−1595.
(88) Lynch, K.; Coffey, A.; Arendt, E. Exopolysaccharide producing lactic acid bacteria: Their techno-functional role and potential application in gluten-free bread products. *Food Res. Int.* **2018**, *110*, 52−61.
(89) Prete, R.; Alam, M. K.; Perpetuini, G.; Perla, C.; Pittia, P.; Corsetti, A. Lactic Acid Bacteria Exopolysaccharides Producers: A Sustainable Tool for Functional Foods. *Foods* **2021**, *10*, 1653.
(90) Jeddou, K. B.; Chaari, F.; Maktouf, S.; Nouri-Ellouz, O.; Helbert, C. B.; Ghorbel, R. E. Structural, functional, and antioxidant properties of water-soluble polysaccharides from potatoes peels. *Food Chem.* **2016**, *205*, 97−105.
(91) Oliveira, T. Í. S.; Rosa, M. F.; Ridout, M. J.; Cross, K.; Brito, E. S.; Silva, L. M.; Mazzetto, S. E.; Waldron, K. W.; Azeredo, H. M. Bionanocomposite films based on polysaccharides from banana peels. *Int. J. Biol. Macromol.* **2017**, *101*, 1−8.
(92) Quilez-Molina, A. I.; Oliveira-Salmazo, L.; Amezúa-Arranz, C.; López-Gil, A.; Rodríguez-Pérez, M. A. ·. Evaluation of the acid hydrolysis as pre-treatment to enhance the integration and functionality of starch composites filled with rich-in-pectin agri-food waste orange peel. *Ind. Crops Prod.* **2023**, *205*, 117407.
(93) Almeida, P. V.; Gando-Ferreira, L. M.; Quina, M. J. Biorefinery perspective for industrial potato peel management: technology readiness level and economic assessment. *J. Environ. Chem. Eng.* **2023**, *11*, 110049.
(94) Al-Sahlany, S. T. G.; Al-musafer, A. M. S. Effect of substitution percentage of banana peels flour in chemical composition, rheological characteristics of wheat flour and the viability of yeast during dough time. *J. Saudi Soc. Agric. Sci.* **2020**, *19*, 87−91.
(95) Manthei, A.; Elez-Martínez, P.; Soliva-Fortuny, R.; Murciano-Martínez, P. Prebiotic potential of pectin and cello-oligosaccharides from apple bagasse and orange peel produced by high-pressure homogenization and enzymatic hydrolysis. *Food Chem.* **2024**, *435*, 137583.
(96) Sampaio, S. L.; Petropoulos, S. A.; Alexopoulos, A.; Heleno, S. A.; Santos-Buelga, C.; Barros, L.; Ferreira, I. C. Potato peels as sources of functional compounds for the food industry: A review. *Trends Food Sci. Technol.* **2020**, *103*, 118−129.
(97) Zhang, J.; Wang, Y.; Yang, B.; Li, Y.; Liu, L.; Zhou, W.; Zheng, S. J. Profiling of Phenolic Compounds of Fruit Peels of Different Ecotype Bananas Derived from Domestic and Imported Cultivars with Different Maturity. *Horticulturae* **2022**, *8*, 70.
(98) Liu, Y.; Gu, Q.; Ofosu, F. K.; Yu, X. Production, structural characterization and gel forming property of a new exopolysaccharide produced by Agrobacterium HX1126 using glycerol or d-mannitol as substrate. *Carbohydr. Polym.* **2016**, *136*, 917−922.
(99) Kamsonlian, S.; Suresh, S.; Majumder, C. B.; Chand, S. Characterization of banana and orange peels: biosorption mechanism. *Int. J. Sci. Technol. Manag.* **2011**, *2*, 1−7.
(100) Mohd Zaini, H.; Roslan, J.; Saallah, S.; Munsu, E.; Sulaiman, N. S.; Pindi, W. Banana peels as a bioactive ingredient and its potential application in the food industry. *J. Funct. Food* **2022**, *92*, 105054.
(101) Radha, D.; Lal, J. S.; Devaky, K. S. Release studies of the anticancer drug 5-fluorouracil from chitosan-banana peel extract films. *Int. J. Biol. Macromol.* **2024**, *256*, 128460.
(102) Chandrasekar, C. M.; Krishnamachari, H.; Farris, S.; Romano, D. Development and characterization of starch-based bioactive thermoplastic packaging films derived from banana peels. *Carbohydr. Polym. Technol. Appl.* **2023**, *5*, 100328.
(103) Lopes, J.; Goncalves, I.; Nunes, C.; Teixeira, B.; Mendes, R.; Ferreira, P.; Coimbra, M. A. Potato peel phenolics as additives for developing active starch-based films with potential to pack smoked fish fillets. *Food Packag. Shelf Life* **2021**, *28*, 100644.
(104) Sucheta; Rai, S. K.; Chaturvedi, K.; Yadav, S. K. Evaluation of structural integrity and functionality of commercial pectin based edible films incorporated with corn flour, beetroot, orange peel, muesli and rice flour. *Food Hydrocolloids* **2019**, *91*, 127−135.
(105) Li, P.; Xia, J. l.; Shan, Y.; Nie, Z. y.; Wang, F. r.; Nie, Z.; yuan; Wang, F. Effects of Surfactants and Microwave-assisted Pretreatment of Orange Peel on Extracellular Enzymes Production by Aspergillus japonicus PJ01. *Appl. Biochem. Biotechnol.* **2015**, *176*, 758−771.
(106) Ma, Y.; Zhao, H.; Ma, Q.; Cheng, D.; Zhang, Y.; Wang, W.; Wang, J.; Sun, J. Development of chitosan/potato peel polyphenols nanoparticles driven extended-release antioxidant films based on potato starch. *Food Packag. Shelf Life* **2022**, *31*, 100793.
(107) Toprakçı, İ.; Balci-Torun, F.; Deniz, N. G.; Ortaboy, S.; Torun, M.; Şahin, S. Recovery of citrus volatile substances from orange juice waste: Characterization with GC-MS, FTIR, 1H- and 13C-NMR spectroscopies. *Phytochem. Lett.* **2023**, *57*, 177−184.
(108) Ghasemlou, M.; Khodaiyan, F.; Oromiehie, A. Rheological and structural characterisation of film-forming solutions and biodegradable edible film made from kefiran as affected by various plasticizer types. *Int. J. Biol. Macromol.* **2011**, *49*, 814−821.
(109) Salazar, D.; Arancibia, M.; Casado, S.; Viteri, A.; López-Caballero, M. E.; Montero, M. P. Green Banana (Musa acuminata AAA) Wastes to Develop an Edible Film for Food Applications. *Polymers* **2021**, *13*, 3183.
(110) de Paula Herrmann, P. S.; Yoshida, C. M. P.; Antunes, A. J.; Marcondes, J. A. Surface evaluation of whey protein films by atomic force microscopy and water vapour permeability analysis. *Packag. Technol. Sci.* **2004**, *17*, 267−273.
(111) Sangeetha, M.; Madhan, D. Corrosion Inhibition of Hydrophobic Nano Film of Eco Friendly Banana peel Extract on Mild Steel in Seawater. *Pharma Chem.* **2021**, *13* (11), 63−70.
(112) Zhang, W.; Li, X.; Jiang, W. Development of antioxidant chitosan film with banana peels extract and its application as coating in maintaining the storage quality of apple. *Int. J. Biol. Macromol.* **2020**, *154*, 1205−1214.
(113) Alancherry, S.; Bazaka, K.; Jacob, M. V. RF Plasma Polymerization of Orange Oil and Characterization of the Polymer Thin Films. *J. Polym. Environ.* **2018**, *26*, 2925−2933.
(114) Aguilar-Sánchez, R.; Munguía-Pérez, R.; Reyes-Jurado, F.; Navarro-Cruz, A. R.; Cid-Pérez, T. S.; Hernández-Carranza, P.; Beristain-Bauza, S. d. C.; Ochoa-Velasco, C. E.; Avila-Sosa, R. Structural, Physical, and Antifungal Characterization of Starch Edible Films Added with Nanocomposites and Mexican Oregano (Lippia berlandieri Schauer) Essential Oil. *Molecules* **2019**, *24*, 2340.
(115) Fonseca, L. M.; Henkes, A. K.; Bruni, G. P.; Viana, L. A. N.; de Moura, C. M.; Flores, W. H.; Galio, A. F. Fabrication and Characterization of Native and Oxidized Potato Starch Biodegradable Films. *Food Biophys.* **2018**, *13*, 163−174.
(116) Farajpour, R.; Emam Djomeh, Z.; Moeini, S.; Tavakolipour, H.; Safayan, S. Structural and physico-mechanical properties of potato

https://doi.org/10.1021/acsomega.4c05924
ACS Omega 2024, 9, 42970−42989

starch-olive oil edible films reinforced with zein nanoparticles. *Int. J. Biol. Macromol.* **2020**, *149*, 941−950.
(117) Plazas, S.; Olaya, C.; Perez, T. Y.; Rodriguez, S.; Mazonas, R.; Ortiz, H.; Rincón, J. A. Síntesis y Caracterización de Biopolímeros Inhibidores de Hongos mediante Microscopia SEM y AFM. *Revista Informador Técnico.* **2016**, *80*, 95−97.
(118) Calle, R. M.; De Los Santos, L.; Bustamante, A.; Angulo, J.; Barnes, C. H. W. Cristalización y morfología superficial de películas delgadas de Ag/SiO 2 tratadas térmicamente. *Rev. Investig. Fis.* **2015**, *18*, 1−9.
(119) Wang, Y.; Zhang, R.; Ahmed, S.; Qin, W.; Liu, Y. Preparation and Characterization of Corn Starch Bio-Active Edible Packaging Films Based on Zein Incorporated with Orange-Peel Oil. *Antioxidants* **2019**, *8*, 391.
(120) Nouri, L.; Mohammadi Nafchi, A. Antibacterial, mechanical, and barrier properties of sago starch film incorporated with betel leaves extract. *Int. J. Biol. Macromol.* **2014**, *66*, 254−259.
(121) Aloui, H.; Khwaldia, K.; Sánchez-González, L.; Muneret, L.; Jeandel, C.; Hamdi, M.; Desobry, S. Alginate coatings containing grapefruit essential oil or grapefruit seed extract for grapes preservation. *Int. J. Food Sci. Technol.* **2014**, *49* (4), 952−959.
(122) Kanmani, P.; Rhim, J. W. Development and characterization of carrageenan/grapefruit seed extract composite films for active packaging. *Int. J. Biol. Macromol.* **2014**, *68*, 258−266.
(123) Synowiec, A.; Gniewosz, M.; Kraśniewska, K.; Przybył, J. L.; Bączek, K.; Węglarz, Z. Antimicrobial and antioxidant properties of pullulan film containing sweet basil extract and an evaluation of coating effectiveness in the prolongation of the shelf life of apples stored in refrigeration conditions. *Innov. Food Sci. Emerg. Technol.* **2014**, *23*, 171−181.
(124) Yang, G.; Yue, J.; Gong, X.; Qian, B.; Wang, H.; Deng, Y.; Zhao, Y. Blueberry leaf extracts incorporated chitosan coatings for preserving postharvest quality of fresh blueberries. *Postharvest Biol. Technol.* **2014**, *92*, 46−53.
(125) Ferreira, A. S.; Nunes, C.; Castro, A.; Ferreira, P.; Coimbra, M. A. Influence of grape pomace extract incorporation on chitosan films properties. *Carbohydr. Polym.* **2014**, *113*, 490−499.
(126) Gniewosz, M.; Synowiec, A.; Kraśniewska, K.; Przybył, J. L.; Bączek, K.; Węglarz, Z. The antimicrobial activity of pullulan film incorporated with meadowsweet flower extracts (Filipendulae ulmariae flos) on postharvest quality of apples. *Food Control* **2014**, *37*, 351−361.
(127) Kanmani, P.; Rhim, J. W. Antimicrobial and physical-mechanical properties of agar-based films incorporated with grapefruit seed extract. *Carbohydr. Polym.* **2014**, *102*, 708−716.

https://doi.org/10.1021/acsomega.4c05924
ACS Omega 2024, 9, 42970−42989